Pressure relief valve sizing: A review of the impact of thermodynamic property method selection and numerical algorithms applied in industrial process design

by

Sefenyiwe Manthata

B.S., University of the Witwatersrand, 2004

A REPORT

submitted in partial fulfillment of the requirements for the degree

MASTER OF SCIENCE

Tim Taylor Department of Chemical Engineering
Carl R. Ice College of Engineering

KANSAS STATE UNIVERSITY
Manhattan, Kansas

2020

Approved by:

Major Professor
Dr Jennifer Anthony

Copyright

Abstract

Pressure relief devices (PRDs) are essential to ensure safe design and operation of most chemical processes ranging from chemical facilities, refineries and pharmaceutical facilities. PRDs are used as overpressure protection devices to avoid vessel or equipment rupture and subsequent uncontrolled loss of containment of process material. The most common type of PRD is the pressure relief valve (PRV). The design of PRVs' is governed (industrial practice) by guidelines set out by several professional bodies that include the American Society of Mechanical Engineers (ASME), American Petroleum Institute (API) and National Boiler Code (NBI).

The study explored the impact of two factors that typically influence the calculation of an appropriate size of a PRV. The factors include the selection of a property method (equation of state) to predict the system physical properties, and the algorithms that are applied to calculate the PRV orifice size. Three cubic equations of state (Peng-Robinson, Redlich-Kwong and Soave Redlich Kwong) were compared, relative to the ideal gas equation of state

The predicted physical properties were applied to two different methods of calculating the mass flux (and subsequently the rated flow capacity) through the pressure relief valve orifice. The methods included a rigorous numerical method (direct integration method) and an empirical formula (API simplified method) to calculate the pressure relief valve orifice size to satisfy the required relief rate.

The study was based on a vapor discharge stream from an ethylene oxide synthesis reactor. The following observations were noted form the results of the study

1. The relative deviation of mass flux prediction (and subsequently pressure relief valve orifice size) ranges between 1% and 7% for all cubic equations of state, relative to the ideal gas equation. The largest relative deviation from ideal gas conditions was demonstrated by the Peng-Robinson equations of state. The trend was consistent for both relief valve sizing methods.

2. The relative difference between the mass flux predicted using the simplified API method and the direct integration method ranged between 54% and 39%. The largest relative deviation was noted for the ideal gas equation of state, whilst the lowest relative difference was noted for the Peng-Robinson equation of state.

3. The relative difference between the mass flux for each of the cubic equations of state is within a range of 0.95% and 0.07%. The largest difference is between Peng-Robinson and Redlich-Kwong equation of state, whilst the smallest difference is between the Redlich-Kwong and Soave-Redlich-Kwong equations of state.

4. The application of the cubic equations of state with either of the PRV orifice sizing algorithms yields a narrow range of orifice sizes. The range is sufficiently small such that one commercial size of orifice is sufficient for all cases (orifice size G).

5. The application of the ideal gas equation of state and the API simplified method, demonstrated significant deviation (relative to the cubic equations of state) for the prediction of the required PRV orifice size. The calculated PRV size is one commercial size smaller that the size predicted using the cubic equations of state. This error is significant because relative orifice area difference for the adjacent commercial sizes is in excess of 35%.

The results suggest that the pressure relief valve sizing algorithm has a significant impact on the selection of a pressure relief valve, and this effect is magnified when ideal gas assumptions are applied for a non-ideal gas. This practice may lead to the selection of a relief valve with an orifice size that is significantly smaller than the required size.

The risk of an inappropriately sized relief valve is significant, as it could lead to valve spring oscillation due to an imbalance in forces at the orifice. This phenomenon is defined as cycling or chattering in industry. This behavior has been synonymous with valve spring failure which could either wedge the relief valve permanently open or closed and lead to a prolonged loss of containment or excessive pressure accumulation respectively. However, if the correct relief valve sizing algorithm is selected, the cubic equations of state predict pressure relief valve orifice sizes that are virtually identical.

The Peng-Robinson equation of state demonstrated the highest relative deviation from ideal gas conditions amongst all the cubic equations of state that were evaluated. This observation is consistent for both mass flux prediction algorithms that were applied.

Furthermore, the Peng-Robinson cubic equation of state includes the most non-zero parameters that are applied to the general form of all cubic equations of state. In the absence of pressure volume and temperature (P, V, T) experimental data for the selected ethylene oxide system, the absolute accuracy of each cubic equation of state could not be determined.

 However, similar comparisons of cubic equations of state have been conducted with similar compounds (polar, non-polar and associative) in comparison to experimental (P,V,T) data. The results of such assessments for similar compounds highlight a consistent pattern, whereby polar compounds reflect a generally lower error in the average relative deviation (%) for predicting the saturated vapor volume and vapor pressure when applying the Peng-Robinson predicted thermodynamic properties.

This observation suggests a correlation between the extent of deviation from ideal gas assumptions for real gases under high pressure non ideal conditions and the relatively higher accuracy of the Peng-Robinson cubic equation of state for compounds of similar molecular structure. This is primarily because the Peng-Robinson equation of state demonstrates two attributes that include; the highest relative deviation from ideal gas equations of state and the lowest deviation from real P, V, T data for similar polar compounds.

However, in order to definitively distinguish the cubic equations of state based on accuracy, system specific P, V, T data would be required because the system parameters for each cubic equation of state are dependent on the species and the thermodynamic conditions of the system.

The study has however provided some insight on the validity of the general limitations that arise due to the polarity of the molecules (molecular structure) and the algorithms that are applied to appropriately select a pressure relief device size (direct integration method vs the API simplified method). Such correlations are generally applied in the process design of pressure relief devices.

For the ethylene oxide system selected, the results demonstrate a relatively small variance between the PRV size estimation based on the cubic equations of state. However, the most significant factor is the relief size estimation algorithm. The API simplified method demonstrates significant limitation when applied to real gas systems, due to the inherent compressibility factor range limitation that it is known to be applicable.

Table of Contents

List of Figures

List of Tables

List of Abbreviations

DEG	Diethylene Glycol
EO	Ethylene Oxide
EoS	Equation of State
BWR	Benedict-Webb-Rubin
MEG	Mono Ethylene Glycol
SRK	Soave-Redlich-Kwong
PR	Peng-Robinson
RK	Redlich-Kwong
P	Pressure
PRV	Pressure Relief Valve
PRD	Pressure Relief Device
PVRV	Pressure Vacuum Relief Valve
V	Volume
T	Temperature
TEG	Triethylene Glycol
S	Entropy
$\underline{S}$	Entropy per mol
U	Internal Energy
$\underline{U}$	Internal Energy per mol
H	Enthalpy
$\underline{H}$	Enthalpy per mol
KE	Kinetic Energy
PE	Potential Energy
Pr	Reduced Pressure
Tr	Reduced Temperature
$\hat{V}$	Specific Volume (Volume per unit mass)
$\underline{V}$	Volume per mol

ΔV-L	Average relative deviation (%) in saturated liquid volume
ΔV-V	Average relative deviation (%) in saturated vapor volume
ΔP-S	Average relative deviation (%) in vapor pressure
PRD	Pressure Relief Device
PRV	Pressure Relief Valve
PVRV	Pressure Vacuum Relief Valve
P_O	Pressure at Stagnant Conditions
V_O	Specific volume at stagnant conditions
VLE	Vapor Liquid Equilibrium

Acknowledgements

I hereby acknowledge the guidance and assistance of my major professor (Dr. Jennifer Anthony).

Her insight on the topic of Advanced Thermodynamics was instrumental to the path I followed to

formulate the master's report, to which I am grateful for.

Dedication

This masters report represents the culmination of years of sacrifice and dedication which would have yielded no fruit in the absence of the Almighty God. I am eternally grateful for his blessings through this journey. He has blessed me with an amazing family. My wife (Sibongile) who has been an anchor of support, assistance, love and my biggest motivator, through some of the most trying times (and in this journey). I have grown with her spiritually, physically and emotionally over many years and I deeply cherish her. My children (Lesedi, Khutso, Kgaugelo and Tumelo) who have been absolutely loving and understanding throughout this journey. My family has sacrificed valuable quality time with me and my full attention during this period and to them I am eternally grateful.

I also want to thank the Almighty God for the blessing in my parents (Thomas and Barbara Manthata) and Grandparents (Rebecca and Phillip Matthews, Mangwato and Mmamodu Manthata) for the foundation, love, support and nurturing they gave to me and my family and the intestinal fortitude and fear of God they have instilled in me through their lived experiences and prayers over many years and on this journey (I am eternally grateful to them).

They endured harsh sacrifices to afford me and my siblings (Khumoestile and Goitseone Manthata) and the greater community, a better life in the midst of brutal repression under the Apartheid regime, in South Africa (my country of birth). I am also eternally grateful to my siblings for the love and support over the years.

Chapter 1 - Selection of thermodynamics models

1.1. Introduction

Pressure relief devices (PRDs) are essential components that ensure safe design and operation of most chemical processes ranging from chemical facilities, refineries and pharmaceutical facilities. Overpressure protection devices (such as PRDs) are installed to avoid vessel or equipment rupture and subsequent uncontrolled loss of containment of process material. The common types of PRDs that are used for over pressure protection of equipment utilized in the chemical manufacturing industry include rupture disks (RD) pressure relief valves (PRV) and pressure vacuum relief valves (PVRV). The design of the PRD's is governed in industrial practice by guidelines set out by several bodies that include the American Society of Mechanical Engineers (ASME), American Petroleum Institute (API) and National Boiler Code (NBI).

The study will explore the relative impact/ sensitivity associated with selecting an appropriate cubic EoS (relative to the ideal gas EoS) for predicting VLE conditions, and the mass flux algorithm required to calculate the required orifice size of the pressure relief valve (based on isentropic expansion).

The study was based on a vapor discharge stream from an ethylene oxide synthesis reactor. The scope of the study does not include a comparison of the cubic equations based on P,V,T data and is therefore not aimed at establishing the absolute accuracy of each cubic EoS based on the system data. However, the output of the process simulations and calculations could be compared with observations for similar compounds from published literature. This would provide a good basis to explore whether any correlation exists between the extent of deviation of each cubic EoS (relative the ideal gas EoS) and the relative error observed for each cubic EoS for similarly, polar and non-polar compounds

The calculation of the relief valve orifice was based estimated by modelling the flow rate as isentropic expansion of a fluid through a nozzle. This is the foundational basis upon which industrial relief valve sizing is conducted as prescribed by the API 520 guidelines [1]. The subsequent size of the relief valve orifice is influenced by thermodynamic models that estimate

the physical properties of the stream components as a function of pressure, temperature and volume. In addition, the industry guidelines make provision for analytical or numerical solutions for calculating the mass flux through (and subsequently the area) of the relief valve orifice.

The study explored the application of three cubic equations of state. They included the Peng-Robinson, Redlich-Kwong, Soave-Redlich-Kwong equations of state and assessed the relative deviation of each of the equations of state against the ideal gas equation of state.
The other consideration was the calculation methodology for determining the required orifice size. The two methods considered were the API simplified equation (analytical method) and the direct integration method (numerical method). These methods were applied to a sample stream comprising of an aqueous ethylene oxide discharge stream from an ethylene oxide synthesis reactor.

The cases reviewed were based on a fixed required relief rate (10,000 lb/hr) upon which the predicted size of relief valve was based. The intent was to evaluate the predicted relief valve orifice size based on the cubic and ideal equations of state The relief conditions yielded only vapor phase relief, therefore the equations of state were compared as the means of assessing the impact of departure from ideal gas conditions when calculating relief valve orifice sizes.

The relief system under evaluation is primarily a reactor operating at a pressure in excess of 15 psig. The appropriate codes of construction for an unfired pressure vessel at these conditions is ASME Section VIII Div.1[2]. The maximum pressure permitted during emergency relief conditions, is defined as the maximum allowable relief pressure (MARP). The value of the MARP for the system is defined by the following relationship [1].

$$MARP = (1 + \frac{Accumulation}{100}) \times MAWP \qquad (0)$$

where accumulation values are:

10%, For a single PRV

16%, For two PRVs in operation

21%, For Fire Case

MAWP is the Maximum Allowable Working Pressure which is a function of design pressure temperature, material properties and thickness of commercially available material.

The primary objective of the report is to determine the relative impact of the following factors that are known to influence the size of a relief device for a specific system. The factors include, the selection of an equation of state (deviation from ideal fluid conditions) and the relief device sizing algorithm. The scope of the assessment shall be confined to the sizing calculations of the relief valves, where thermodynamic properties are applied to industry guidelines [1][3]. Furthermore, the system conditions are evaluated at elevated pressure (above 10 bar). This is done to filter out the impact of the system conditions since a significant number of equations of state models correlate with the ideal gas assumption at low pressure conditions.

Most ethylene oxide production plants are based on the direct ethylene oxidation process with air or oxygen using a silver-based catalyst. Carbon dioxide (CO_2) and water are produced as by-products of the reaction.

Ethylene oxide (EO) is selectively produced utilizing a silver-based catalyst at 200 to 300 °C and 10-20 bar. Along with ethylene oxide (80-85 %), CO_2, H_2O and heat are generated. Reaction heat is recovered by boiling water at elevated pressure on the reactors shell side.
The overall reaction chemistry can be simplified as [5]:

$$CH_2=CH_2 + 1/2\ O_2 \quad \rightarrow \quad (CH_2CH_2)\ O \qquad \Delta H\ = +101\ Btu/mol \qquad (R1\text{-}a)$$
$$CH_2=CH_2 + 3\ O_2 \quad \rightarrow \quad 2CO_2\ +\ 2H_2O \qquad \Delta H\ = +1254\ Btu/mol \qquad (R1\text{-}b)$$
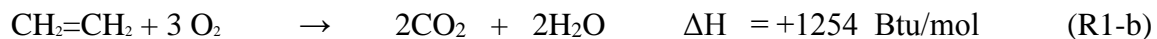
The ethylene oxide process schematic is highlighted below (See Figure 1.1, [4])
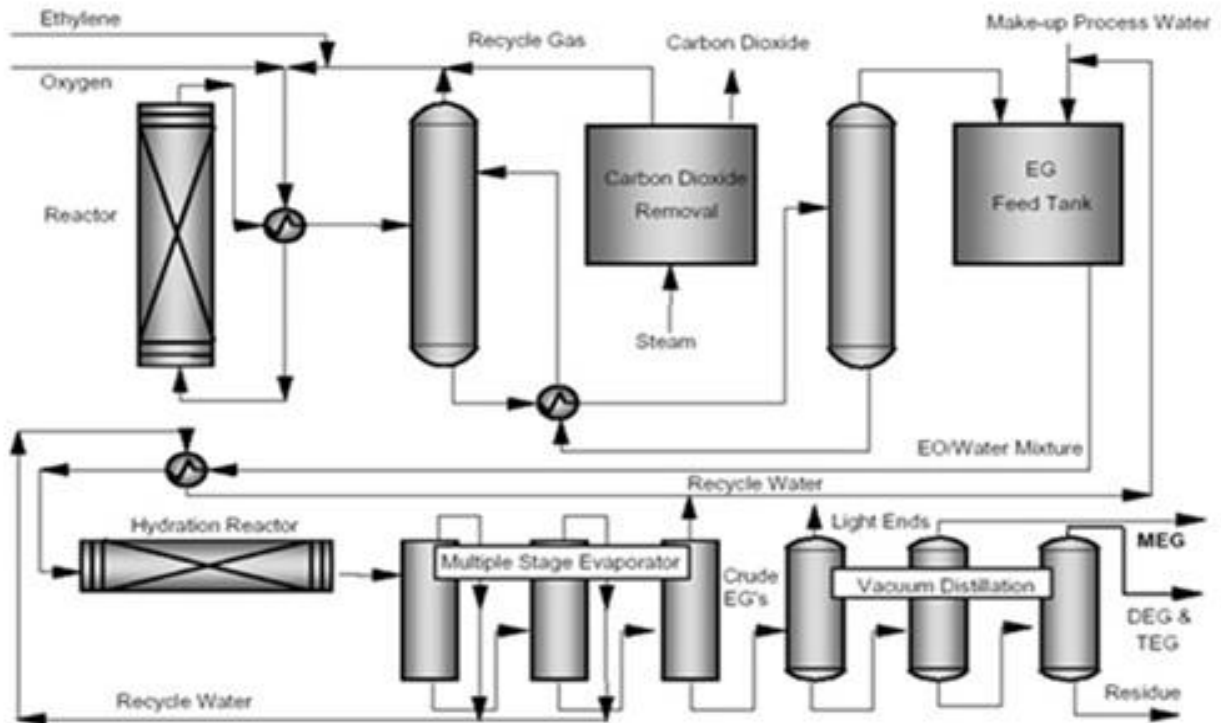
Figure 1.1: Ethylene oxide production process [4]

1.2. Commercial production of ethylene oxide and ethylene glycol

There are two common methods of commercial ethylene glycol production. They include:

- Hydration of ethylene oxide and mono ethylene glycol (MEG)
- Hydrolysis of ethylene oxide in the presence of excess water

Ethylene oxide (EO) is obtained by direct oxidation of ethylene with air or oxygen.

The ethylene oxide is thermally hydrolyzed to ethylene glycol without a catalyst.

monoethylene glycol (MEG), diethylene glycol (DEG), and triethylene glycol (TEG) are also produced, with respectively decreasing yield, and are separated from the ethylene glycol by a series of distillation columns at reduced pressure.

1.2.1. Glycol reaction

Ethylene oxide reacts with water to yield a series of glycols and polyglycols. The stoichiometry of the series of reactions is highlighted below

C_2H_4O + H_2O → $HO-C_2H_4-OH$ (R2)

(EO)   (Water)   (MEG)

C_2H_4O + $HO-C_2H_4-OH$ → $HOCH_2CH_2(OCH_2CH_2)OH$ (R3)

(EO)   (MEG)   (DEG)

C_2H_4O + $2(HO-C_2H_4-OH)$ → $HOCH_2CH_2(OCH_2CH_2)_2OH$ (R4)

(EO)   (DEG)   (TEG)
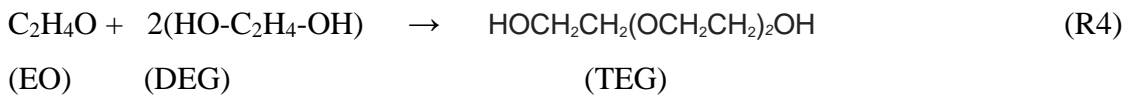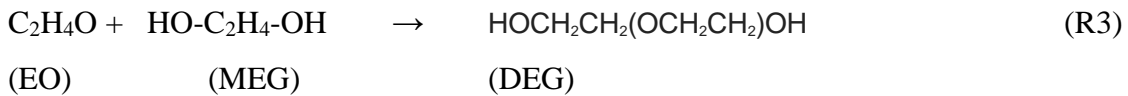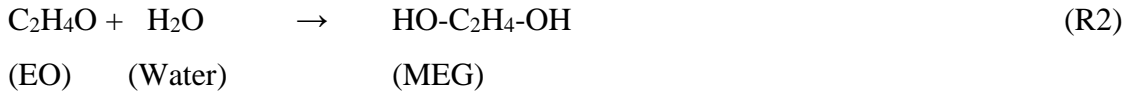
However, the reaction conditions do not enable appreciable formation of glycols. This is because in the reaction unit, the concentration of water in process streams is very low, providing a small driving force for this reaction. Secondly, rust catalyzes this side reaction. Since stainless steel reactor tubes are used, rust is negligible [5].

 In the second method, ethylene glycol is manufactured by the reaction of ethylene oxide with carbon dioxide to form ethylene carbonate, an intermediate product, which can be hydrolyzed to ethylene glycol. This method has now been successfully commercialized by the Shell Group under the process technology name Shell OMEGA (Only MEG Advanced) [6]

The scope of this masters report shall be based on ethylene oxide production via the direct oxidation process. The flowsheet was simulated using Aspen Plus simulation software V10. This process consists of the three main sections (see Figure 1.2) that include the reaction system, the absorption system, and the ethylene oxide purification. The system that has been selected to conduct this review is the gas overhead stream of the reaction system (Vessel R-101).
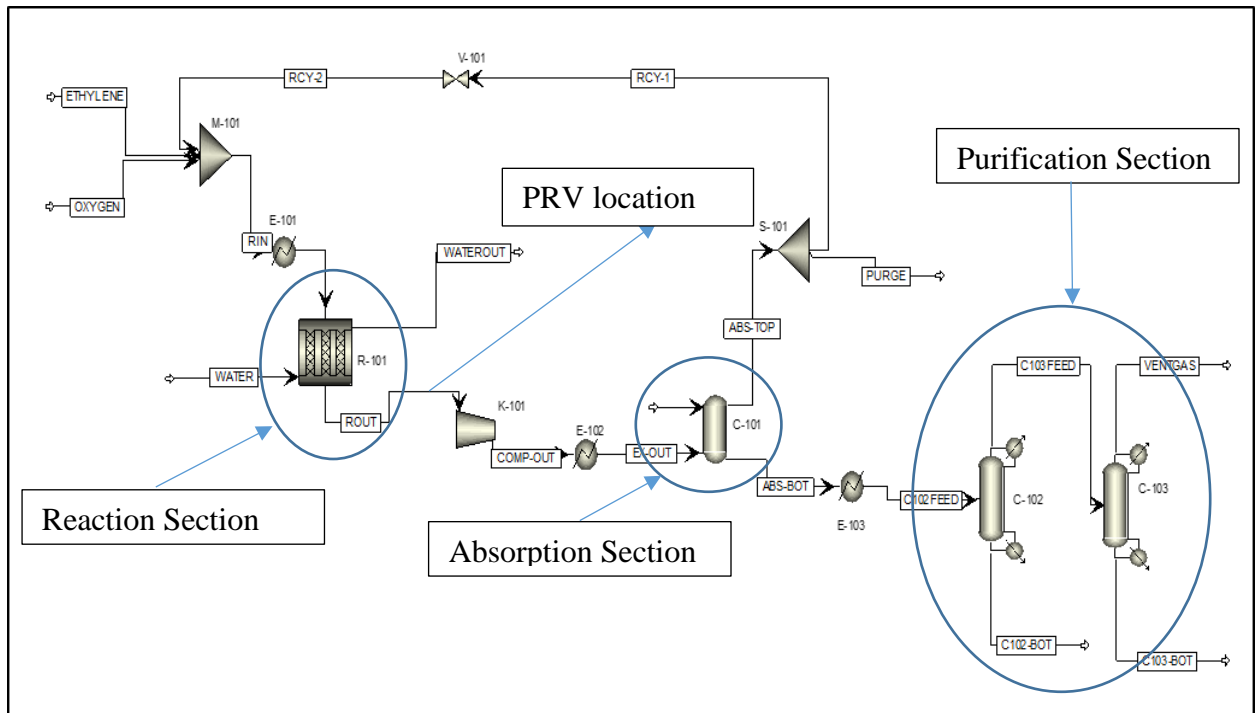
Figure 1.2: Ethylene oxide: Reactor section Aspen Plus simulation

1.2.2. Ethylene oxide reaction section

The reactor section comprises a vertically orientated tubular packed bed reactor. The tubes within the reactor shell contain a silver /alumina catalyst. This reactor design can accommodate high superficial velocities [5] and has subsequently less volume than other reactor designs. The shell and tube design also allow for effective heat transfer between the shell side coolant (water) and the reactions in the packed bed in each reactor tube. This is a crucial design feature because the ethylene oxide synthesis reaction is highly exothermic and has the propensity for the development of hot spots in the reactor. The development of hot spots is known to propagate and initiate catalyst degradation and ultimately thermal runaway reaction temperatures. The effects of thermal runaway temperatures are known to be catastrophic due to the highly exothermic nature of the ethylene oxide reaction.

The feed to the reactor comprises high purity oxygen and ethylene in tandem with a diluent gas. The diluent gas is typically methane and serves the purpose of reducing the concentration of

oxygen in the reactor recycle stream. Excessive oxygen concentration in the reactor recycle could lead to an oxygen rich environment ,which is susceptible to initiating an explosion. The diluent gas is assumed to be inert and therefore its concentration has not been reflected on the discharge and suction side of the reactor streams. The catalyst facilitates the two reactions that include:

- The reaction of ethylene and oxygen to form ethylene oxide
- The complete oxidation of ethylene to form carbon dioxide and water

The design details of a typical ethylene oxide reactor are based on work done by Lou et al [5]. The details are summarized in Table 1.1 and Table 1.2.

Reactors Specifications		
Design Details		
	Operating Conditions	
Process stream		
Pressure (Psig)	221	
Temperature (ºF)	405	
Reactor Outlet Stream Composition		
Ethylene	(lb-mol/hr)	571.8
Ethylene Oxide	(lb-mol/hr)	862.6
Carbon Dioxide	(lb-mol/hr)	717.2
Water	(lb-mol/hr)	162.1
Oxygen	(lb-mol/hr)	2546.7

Table 1.1: Ethylene oxide reactor specifications

Relieving Pressure Calculation		
Operating Pressure	psi	221
Max operating pressure	psi	287.3
MAWP (psi)	psi	350
MARP (psi)	psi	423.5
% Accumulation	%	20

Table 1.2: Ethylene oxide relieving pressure calculation

Chapter 2 - Property method selection

The selection of a property method for a system is highly dependent on the molecular structure of the main constituents of the system. In this case, the major components are ethylene oxide and water. The less significant components include mono ethylene glycol, diethylene glycol and tri ethylene glycol.

2.1. Molecular structure of components.

2.1.1. Ethylene oxide

Ethylene oxide or oxarine is a triangular shaped, cyclic ether (epoxide). It contains two methylene (CH_2) groups and one oxygen atom plus one dipole (see Figure 2.1). The overall charge distribution of the molecule is polar.
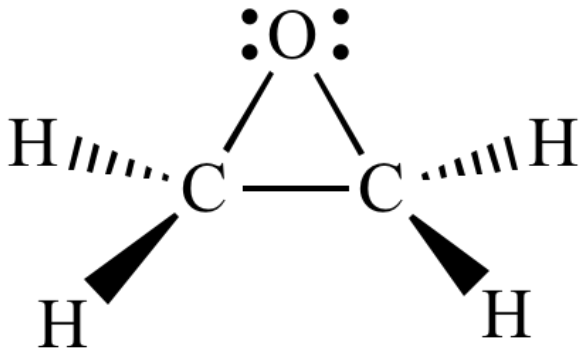
Figure 2.1: Ethylene oxide molecular structure

In the absence of experimental data or limited data, the calculation of thermophysical properties of fluids are undertaken based on molecular models. If the theoretical models resemble the true nature of the intermolecular forces, the accuracy of the thermophysical properties can essentially be used in the place of experimental data. One such approach was evaluated for a six-dimensional potential energy hypersurface for two interacting ethylene oxide molecules. The method adopted was a high-level quantum-chemical ab initio calculation that included a site-site potential function with 19 sites per molecule [7]. The sites are orientated within each molecule according to the following convention:

- One site for each of the seven atoms,

- One site for each of the four C–H bonds (non-polar)

- Two sites along each of the two C–O bonds (polar)

- Two sites along the C–C bond (non-polar)

- Two sites at the positions of the free electron pairs of the oxygen atom

The subsequent orientation renders the sites to be in accordance with the symmetry of the Ethylene oxide molecule. This translates to eight different types of sites and 36 unique permutations of site -site combinations [7].

The intermolecular forces that are prevalent in pure ethylene oxide, in order of bond strength, include:

1. Dipole-Dipole Forces

Dipole-dipole forces arise due to an electrostatic attraction between the dipole moments of two ethylene oxide molecules. The structure of an ethylene oxide molecule lends itself to multiple bonding permutations such that the negative oxygen atom is capable of bonding with the any of the four positively charged hydrogen atoms. (See Figure 2.2)

2. London Dispersion Forces

These forces are characterized as the weak attraction force between molecules.
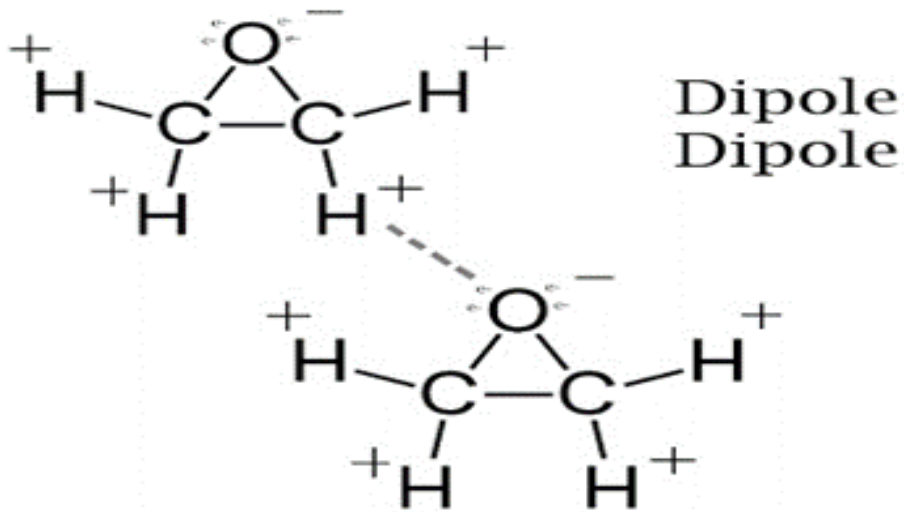
Figure 2.2: Ethylene oxide dipole-dipole forces

3. Ethylene oxide bond angles

   The cyclical structure of ethylene oxide resembles an equilateral triangle with bond angles of approximately 60° and a significant angular strain corresponding to the energy of 105 kJ/mol. [8]. In comparison with other bond angles, the C–O–H angle in alcohols is approximately 110°; in ethers, the C–O–C angle is 120°. Therefore, the acute angles associated with the epoxy cyclic bond leads to a large angular strain and large potential for opening of the cyclic ring.

2.1.2. Ethylene glycol

Ethylene glycol can be characterized as a polar molecule. The intramolecular forces that are prevalent in pure ethylene gylcol molecules include.

- C – O polar; covalent
- H - C non-polar; very covalent
- C - C non-polar; purely covalent

The intermolecular forces present in pure ethylene glycol include dispersion, dipole-dipole, and hydrogen bonds. Hydrogen bonds dominate because ethylene glycol has two alcohol functional groups (-OH), which can form two hydrogen bonds, compared to a single hydrogen bond in the other two-carbon molecules such as ethanol.

2.2.Property method selection process

The methodology for selecting appropriate property methods (for the single gas phase mixture shall be based on the Aspen Plus simulation tool Property selection methodology. The decision map schematic is highlighted below in Figure 2.3 and Figure 2.4 [9])
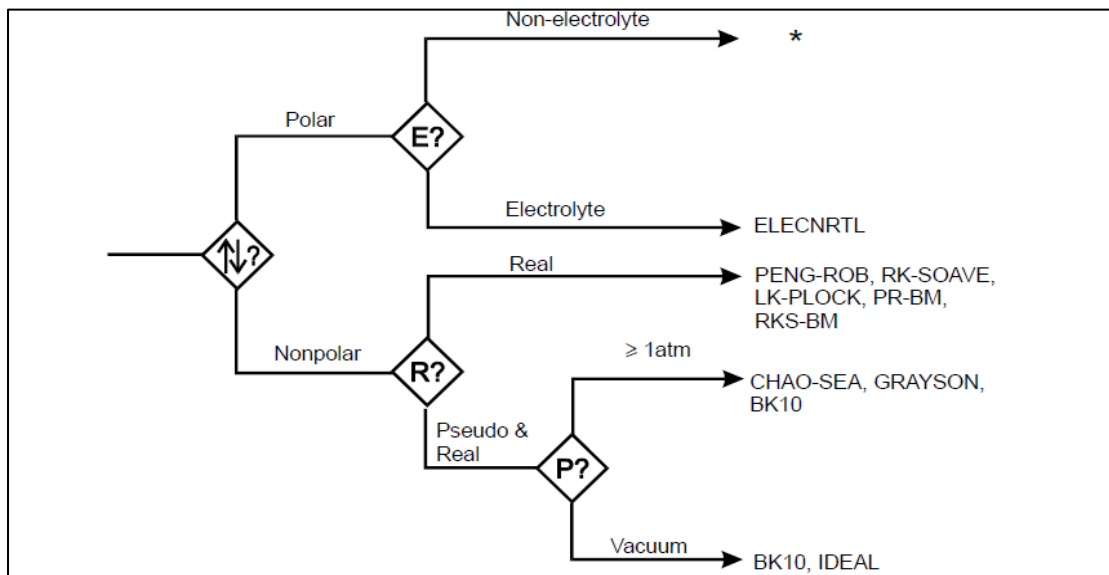
Figure 2.3: Part 1 Aspen Plus equation of state selection logic map [9]

11
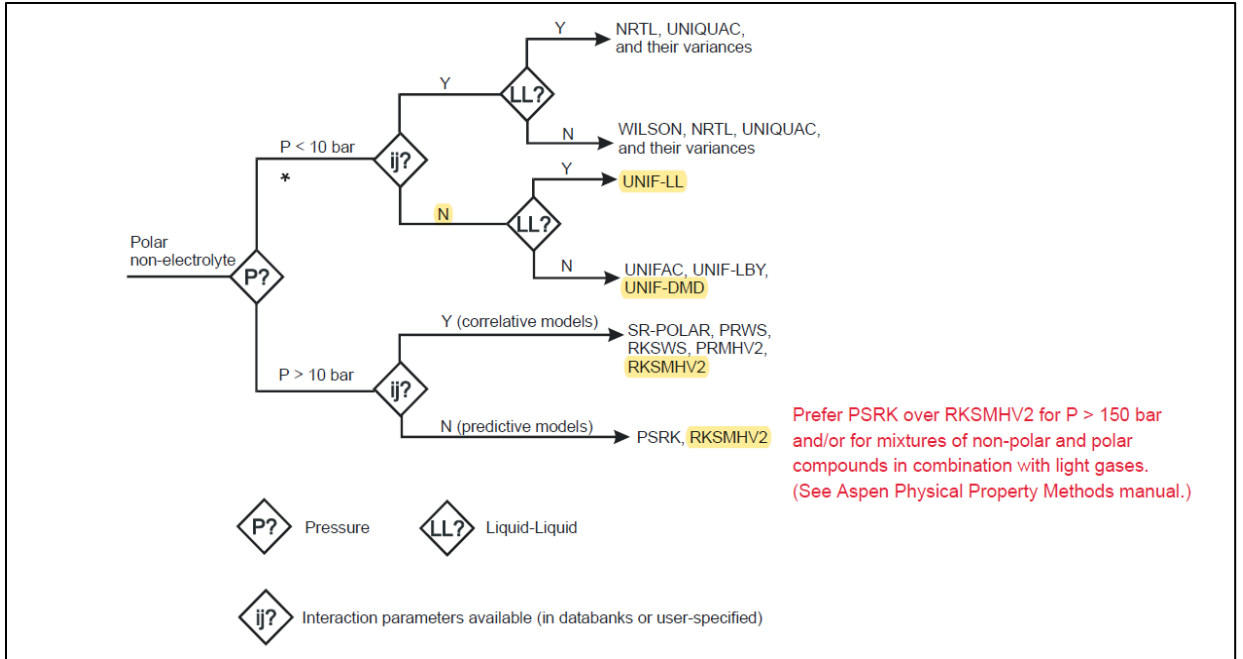
Figure 2.4: Part 2 Aspen Plus equation of state selection logic map [9]

Aqueous ethylene oxide systems are highly nonideal vapor-liquid equilibrium systems [10]. For non-polar compounds at elevated pressures (in excess of 10 bar) and available interaction parameters in the Aspen plus databank. The suggested property method for non-polar compounds includes Peng-Robinson, RK-Soave (see Figure 2.3). For polar, non-electrolyte compounds, at a similarly high pressure the Aspen guideline recommends the use of a variation (of mixing rules) of either the RK-Soave Peng-Robinson EoS (ie PRMHV2 or RKMHV2 respectively).

Literature from similar studies also supports the use of the Peng-Robinson EoS for ethylene oxide / water mixtures. The phase envelope (Figure 2.5) for the aqueous ethylene oxide mixture shows a good fit between the experimental data and the Peng-Robinson EoS predicted data across the range of ethylene oxide /water mixture proportions. However, the data was based on low pressure conditions (1.013bar).
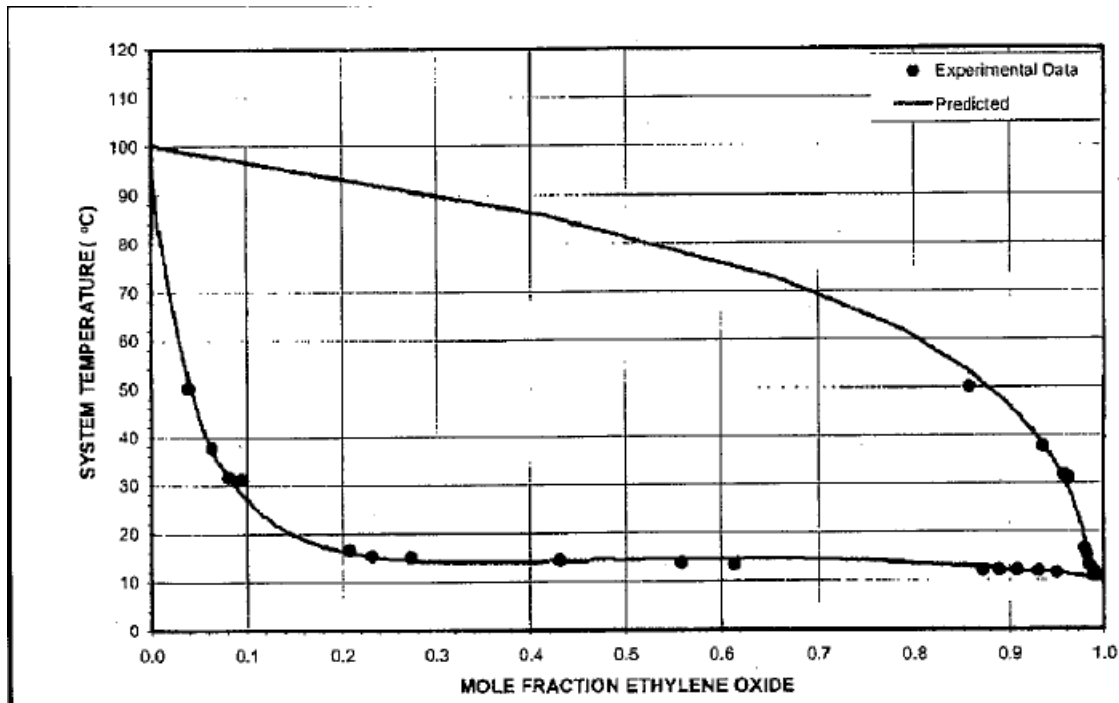
Figure 2.5: Comparison of experimental TXY data and Peng-Robinson equation of state predictions for the ethylene oxide water system at 1.013 bars [10]

2.3. Prediction of fluid behavior: Cubic equations of state

The sizing of pressure relief valves is heavily reliant on the accurate prediction of the intensive properties of the compounds that a system comprises. The two methods that are commonly used to predict the response to pressure volume and temperature, include equations of state or molecular simulations. However, equations of state are the dominant method for predicting the intensive properties for a mixture for the sizing relief valves.

The thermodynamic functions that relate variables such as ($\underline{S}$, $\underline{U}$ and $\underline{V}$) or other combinations such as ($\underline{H}$, $\underline{S}$ and P) are defined as fundamental equations of state. However, there is seldom enough information available to construct fundamental equations of state. The parameters that are available typically include P, $\underline{V}$ and T and can be used to construct relationships called cubic or

13

volumetric equations of state. The earliest form of the cubic equations of state is the van der Waals EoS which was developed by J.D van Der Waal in 1873 [11]

The equation of state departs from ideal gas assumptions by factoring in two significant properties associated with real gases. The first assumption includes the observations that the molecules occupy a volume. This implies that gas molecules do not behave like point charges and do interact with adjacent molecules and the vessel. The collisions, associated with the interactions, cause a change in the kinetic energy of the system.

$$b = \sum_{i=1}^{m}(y_i b_i) \qquad (1)$$

The ideal gas law is based on the assumption that volume (V) occupied by n moles of any gas has a pressure (P) at temperature (T) in degrees Kelvins given by the following relationship, where R is the universal gas constant:

$$P = n\frac{RT}{V} \qquad (2)$$

The volume occupied by a real gas is accounted for through two modifications to the ideal equation. The van der Waals equation replaces *Volume (V)* in the ideal gas law with molar volume (V) of the gas and the term b that is proportional to the size of the molecules [12]

The additional modification to the ideal gas law accounts for the attractive forces between molecules. The term a is commonly used for parameters that are a measure of intermolecular attraction. Van der Waals provided for intermolecular attraction by adding the term a to the observed pressure *P* in the equation of state.

The values of the constants a and b can be determined either by fitting the Van der Waals equation of state to experimental data or from data derived at critical point conditions for pure components. The values of a and b for multicomponent mixtures are estimated utilizing mixing rules.
The simplest form of the mixing rules for calculating term a is derived by assuming that the molecules are spherical. This enables the calculation of an average molecular diameter.

$$b^{\frac{1}{3}} = \sum_{i=1}^{m}\left(y_i b_i^{\frac{1}{3}}\right) \qquad (3)$$

This assumption is effective for similar molecules at moderate densities because the mixing rule used to determine b does not significantly affect the results. However, the mixing rule that is used to determine the *a* term has a significant impact on the estimation of the fugacity of a component in a mixture [13]

The *a* term may be expressed by averaging over all molecular pairs.

$$a = \sum_{i=1}^{m}1\sum_{j=1}^{m}y_i y_j a_{ij} \qquad (4)$$

where

a_{ij} is the measure of the strength of attraction between a molecule i and molecule j.

y_j is the mol fraction of component j.

Where experimental data is not available, the value of a_{ij} for dissimilar mixtures is predicted by the equation

$$a_{ij} = (a_i a_j)^{1/2} \qquad (5)$$

The van der Waals equation of state is the basis of derivation of all cubic equations of state. The general form of all cubic equations of state can be represented [14] as follows:

$$P = \left(\frac{RT}{\widehat{V}-b_i}\right) - \left(\frac{a_i(T)}{(\widehat{V}-r_1 b_i)(\widehat{V}-r_2 b_i)}\right) \qquad (6)$$

where

$$b_i = \Omega_b R \frac{T_{c,i}}{P_{c,i}} \qquad (7)$$

15

$$a_i(T) = \Omega_a R^2 \frac{T_{c,i}^2}{P_{c,i}} \alpha_i(T, T_{c,i}, \omega_i) \tag{8}$$

where

Ω_a, Ω_b are parameters for the cubic equations of state (see Table 2.1)

ω_i is the acentric factor of component i

α_i is the temperature dependence of the energetic parameter

Equation of State	Ωa	Ωb
Redlich-Kwong	0.42747	0.08664
Peng-Robinson	0.45724	0.0778
Van der Waals	0.421875	0.125

Table 2.1: Cubic equation of state Ωa and Ωb terms [22]

r_1 and r_2 are parameters that are applied to the generic form of the cubic equations of state. The specific r parameters for three cubic equations of state are summarized in Table 2.2 below

Equation of State	r1	r2
Van Der waals	0	0
Soave - Redlich-Kwong (SRK)	0	-1
Peng-Robinson	$-1 + \sqrt{2}$	$-1 + \sqrt{2}$

Table 2.2: Cubic equation of state r parameters [13]

The development of cubic equations of state has been based on sequential improvements of preceding equations of state. Figure 2.6 presents a brief chronological sequence of the developments.
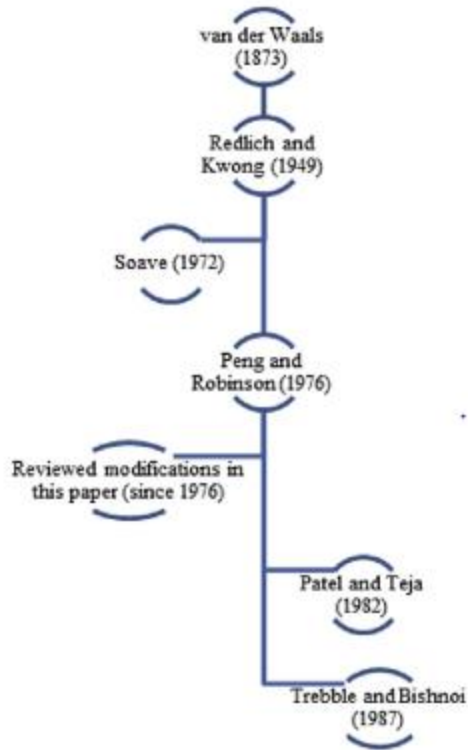
Figure 2.6: Cubic equations of state chronological development [14]

2.3.1. Redlich-Kwong equation of state

In 1949, the most successful modification of the cubic EoS was presented by Redlich and Kwong [14]

$$P = \left(\frac{RT}{\hat{V}-b}\right) - \left(\frac{a(T)}{\hat{V}(\hat{V}+b)T^{1/2}}\right) \tag{9}$$

where

$$a = \frac{R^2 T_c^{5/2}}{9(2^{1/3}-1)P_c} = 0.42748 \, \frac{R^2 T_c^{5/2}}{P_c} \tag{10}$$

$$b = \frac{(2^{1/3}-1)RT_c}{3P_c} = 0.08664 \, \frac{RT_c}{P_c} \tag{11}$$

The Redlich–Kwong equation was designed largely to predict the properties of small, non-polar molecules in the vapor phase, which it generally does well. However, it has been subject to various attempts to refine and improve it.

The noticeable feature of the RK- EoS, included the temperature-dependent cohesion function (a (T)). As it is expected, the a-term (a (Tr)) decreases with an increase in temperature. However, the equation is essentially empirical because its justification is based on the degree of approximation obtained by comparatively simple means.

2.3.2. Soave-Redlich-Kwong equation of state

The modifications made by Soave [15] contributed significant improvements to the prediction of the Redlich-Kwong equation of state by fitting the cohesion function on the vapor pressure at the reduced temperature value of 0.7 (i.e. Tr = 0.7) In addition, a new parameter (α) was added that was a function of temperature and the acentric factor (ω). These modifications were also affected by the molecular structure of the species in the system.

$$P = \left(\frac{RT}{\widehat{V}-b}\right) - \left(\frac{\alpha(Tr,w)a_i\,(T)}{\widehat{V}(\widehat{V}+b)}\right) \qquad (12)$$

where

$$\alpha = (1 + (0.480 + 1.574\omega - 0.176\omega^2)(1 - \sqrt{T_r}))^2 \qquad (13)$$

$$T_r = \frac{T}{Tc} \quad \text{(Reduced temperature)} \qquad (14\text{-}1)$$

$$P_r = \frac{P}{Pc} \quad \text{(Reduced Pressure)} \qquad (14\text{-}2)$$

$$P_r^s \quad \text{(Reduced Saturation Pressure)} \qquad (14\text{-}3)$$

At Tr =0.7 the following universal relationship between Tr and ω
exists, that can be written as

$$[P_r^s]_{\text{at Tr}=0.7} = 10^{-(\omega+1)} \qquad (14\text{-}4)$$

2.3.3. Peng-Robinson equation of state

The Peng Robison EoS was developed based on the premise of improving some of the deficiencies associated with liquid volume prediction by the Soave-Redlich-Kwong equation of state. In general, the liquid volume predicted with the Soave-Redlich-Kwong EoS yields a higher prediction than experimental results [16]. The instances where compounds with a large acentric factor (ω) demonstrated increases in deviation, the behavior may be attributed to the high-fixed value of the critical compressibility factor (Zc) equal to 1/3. The fixed value for the compressibility factor is a restraint imposed by the Redlich-Kwong EoS due to restrictions that apply at the critical point which is imposed by the RK EoS (due to the restrictions at the critical point [17]).

The development of the Peng-Robinson EoS was a departure from the development of the Redlich-Kwong EoS in two significant ways:

- The Van der Waals attractive term structure of the EoS was modified based to improve representation of attractive pressure forces.
- The developers retained rigorous aspects of the Redlich-Kwong EoS (i.e. temperature dependence of the α term).

The subsequent term yielded was:

$$P = \left(\frac{RT}{\widehat{V}-b}\right) - \left(\frac{a_i\,(T)}{\widehat{V}(\widehat{V}+b)+b(\widehat{V}+b)}\right) \tag{15}$$

where

$$\alpha = (1 + k(1 - \sqrt{T_r}))^2 \tag{16}$$

$$a = a_c\alpha \tag{17}$$

$$k = 0.37464 + 1.54226\omega - 0.26992\omega^2 \tag{18}$$

$$a_c = 0.45724\frac{R^2 T^2}{P_c} \tag{19}$$

$$b = 0.0778\frac{RT}{P_c} \tag{20}$$

The Peng-Robinson EoS included a new term to improve the prediction of attractive pressure forces. The new term, $b(\hat{V} + b)$, is included in the EoS expression and it subsequently enhances the ability to predict the liquid phase densities [18].

The other notable attributes of Peng-Robinson include:

- Higher accuracy of predicting saturation pressure and vapor liquid equilibrium
- Better performance at near critical conditions
    - Peng-Robinson: $Zc = 0.307$
    - Soave Redlich-Kwong : $Zc = 0.333$
    - CH_4 compressibility: $Zc = 0.288$
- Better prediction of liquid densities for C5+ and heavier compounds

The comparison of the Peng-Robinson and Soave-Redlich-Kwong EoS revealed strong similarity for gas phase density and enthalpy estimations. This is demonstrated in the reduced pressure and reduced volume graph (Figure 2.7) for n-butane [15]. The graph illustrates the negligible relative difference in the reduced pressure and reduced volume estimation within the temperature range of 350K- 500K.
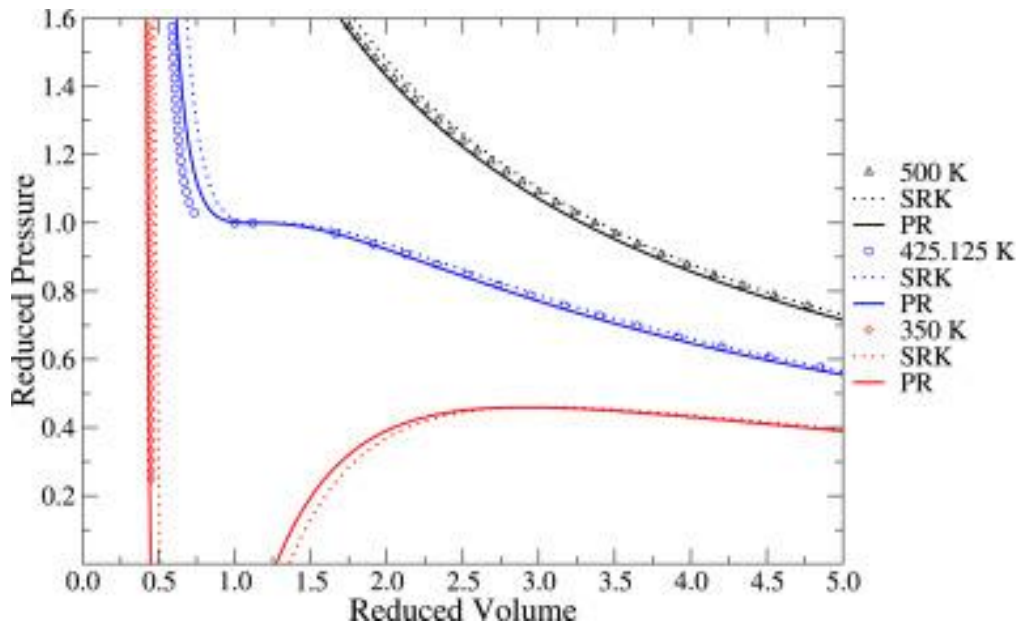
Figure 2.7: Calculated isotherms by PR76 and SRK72 equations of state for n-butane at a higher temperature (500K) and a lower temperature (350K) than critical temperature (425.125K) [15]

However, the deviation appears to be significant when comparing the saturation pressure (Psat) for pure compounds and liquid phase density. Experimental results reported by Perez et al [19] indicate that the Peng-Robinson EoS is more suitable than SRK for estimating density of heavier hydrocarbons (C5+ or higher), aromatic hydrocarbons (toluene and benzene) and SO2. The fugacity coefficients calculated using the Soave Redlich-Kwong equation of state provided better agreement with near experimental results [20], obtained through the modified Benedict-Webb-Rubin (BWR) thermal equation of State [21], when compared with the Peng-Robison equation of state. The cause of the deviation in the Peng-Robinson fugacity coefficient estimation arises from reduction in the compressibility factor (Zc) to a more realistic value in comparison to the Soave Redlich-Kwong equations of state.

Chapter 3 - Conventional relief capacity calculations

The established industry practice for calculating the orifice size required for adequate relief of a pressurized system involves equations developed from two steps.

1. The mass and energy balance around the source of overpressure (i.e. the vessel and associated piping.

2. The flow capacity across the pressure relief device (i.e. the pressure relief valve)

The first step determines the system capacity that the relief valve shall encounter on the suction side, whilst the second step shall determine the required orifice size in order to achieve the required relief rate. The significant assumption upon which the industry methodology is based (API -520 Part 2) [1] includes, reversible and adiabatic expansion which is known as an Isentropic process.

3.1. Dynamic mass and energy balances

Dynamic differential mass balance across the source of mass flow to the relief valve is depicted in system as presented in Figure 3.1
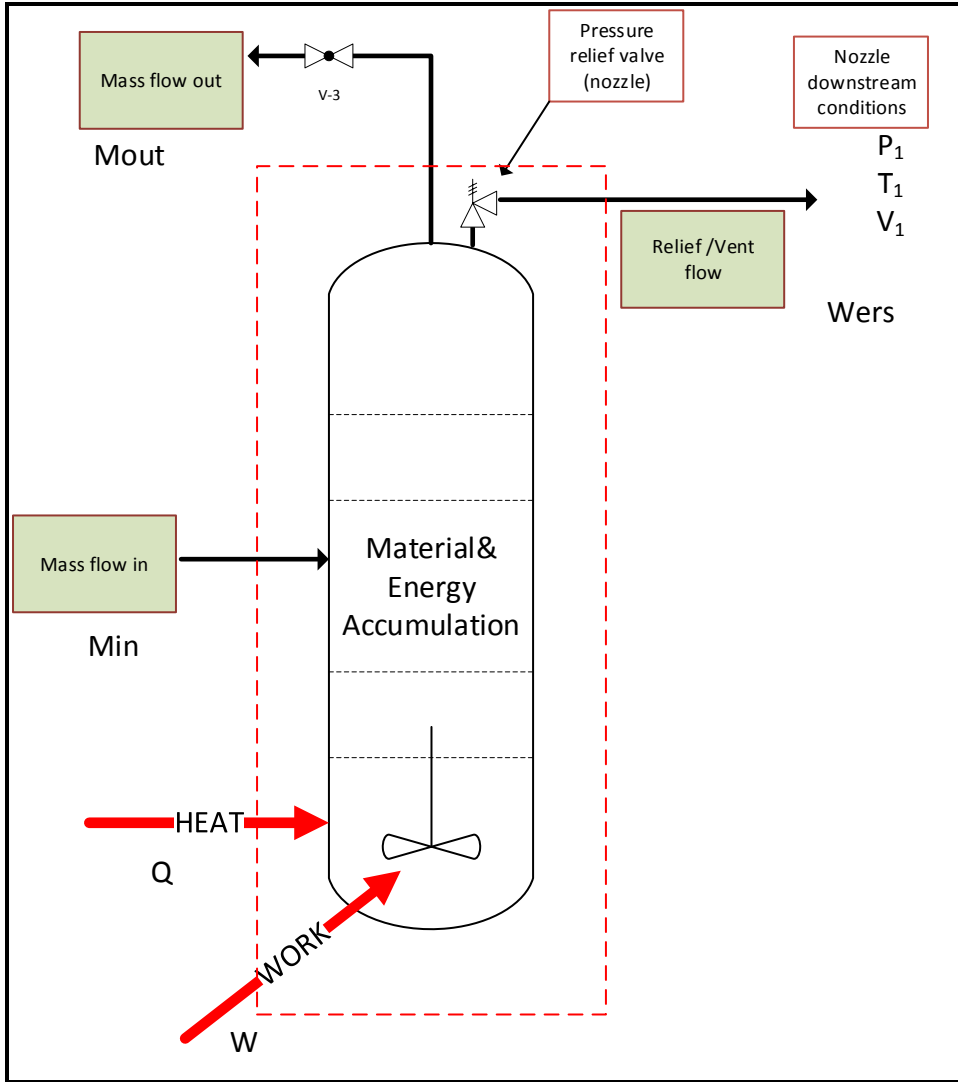
Figure 3.1: Dynamic differential mass and energy balance across the system

Mass balance

$$\frac{dM_{Total}}{dt} = \sum \dot{M}_\iota = \dot{M}_F - \dot{M}_{out} - \dot{W}_{ERS} \tag{21}$$

$$M_{Total} = M_{Vessel} + M_{Solids} + M_{Liquid} + M_{Vapor} \tag{22}$$

Energy balance

$$\frac{dE_{Total}}{dt} = \dot{Q} + \dot{W} + \sum \dot{M}_\iota \widehat{E}_\iota \tag{23}$$

$$E_{Total} = E_{Vessel} + E_{Solids} + E_{Liquid} + E_{vapor} \tag{24}$$

$$E_{Total} = U + KE + PE \tag{25}$$

$$H = U + PV \tag{26}$$

where

$\dot{M}_i$ is the mass flow rate of component i (lb/hr)

$\dot{M}_F$ is the feed mass flow rate (lb/br)

$\dot{M}_{out}$ is the over head discharge mass flow rate (lb/hr)

$\dot{W}_{ERS}$ is the PRV discharge mass flow rate (lb/br)

M_{Total} is the total mass of the system (lb)

M_{Solids} is the mass of solids in the reactor (lb)

M_{Liquid} is the mass of the liquid in the rectaor (lb)

M_{Vapor} is the mass of the vapor in the reactor (lb)

M_{Vessel} is the thermal mass of reactor vessel (lb)

$\dot{Q}$ is the heat input to the reactor (Btu/hr)

$\dot{W}$ is the hydraulic work (shaft work) input to the reactor (Btu/hr)

$\hat{E}_i$ is the energy input per unit mass for component i associated with the stream

material flow (Btu/lb)

E_{Total} is the total system energy (Btu)

E_{Solids} is the energy of solids in the reactor (Btu)

E_{Liquid} is the energy of the liquid in the reactor (Btu)

E_{Vapor} is the energy of the vapor in the reactor (Btu)

E_{Vessel} is the energy of the reactor vessel metal (Btu)

24

The assumptions that are relevant to the relief system, include:

- Thermal mass of reactor vessel is negligible (M_{Vessel})

- Potential Energy (PE), Kinetic Energy (KE) terms are negligible

- Work term for stirrer $\dot{W}$ is negligible

- Normal discharge flow $\dot{M_{out}}$ is Negligible during a relief event most flow is diverted to the relief valve vent

- System is at pseudo steady state

The basis of the mass flow rate on the overhead discharge line form the reactor was the abovementioned assumptions. The mass flow rate shall be set as the mass flow rate that discharges through the pressure relief valve.

3.2. Pressure relief valve flow capacity calculation

The orifice size of the pressure relief valve shall be determined by the mass flux through the valve. The mass flux equation is derived from a momentum balance and for isentropic nozzle flow of a homogenous fluid. The formula applies to both two phase and single-phase flow. The overhead discharge line from the pressure relief valve shall be single phase vapor

The derivation of the nozzle mass flux equation is based on the assumption of adiabatic and frictionless flow through a nozzle. The momentum balance equation is also applied to the flow through the nozzle (see equation 27)

$$\hat{V}dP + d\left(\frac{\hat{V}^2}{2gc}\right) + \frac{g}{gc} * \frac{dz}{dx} + 4 * \frac{f}{Dx} * \frac{\hat{V}^2}{2*gc} * \text{dx} = 0 = Td\hat{S} + \hat{V}dP \qquad (27)$$

Assumptions

1. No elevation changes

2. Frictionless flow in the Nozzle

The entropy balance applied across the nozzle.

$$dS = \frac{dQ}{T} = 0 \qquad (28)$$

Assumption

1. Adiabatic conditions

The subsequent expression can be simplified to an indefinite integral expression (see below).

$$d\left(\frac{\hat{V}^2}{2gc}\right) = -\hat{V}dP \qquad (29)$$

When the indefinite integral was assessed at stagnant conditions (in the reactor) through to the PRV nozzle outlet conditions (uo, Po) and (u,P) respectively. The integrated mass flux expression is:

$$G = \frac{1}{v}\left[-2g_C \int_{p_0}^{p} V dp\right] \tag{30}$$

The energy balance for isentropic expansion is applicable irrespective of the non-ideality or the compressibility of the fluid. Therefore, the equation applies to two phase and single-phase conditions.

The upper and lower limits of integration are the pressure upstream (inlet nozzle) to the relief valve and the downstream (discharge line) pressure. The integration can be executed numerically or analytically. Either of the methods requires that the density at inlet conditions be known as a starting point. The equation represents the ideal mass flux that has not been corrected for the co-efficient of discharge, back pressure correction factor, and the viscosity correction factor. For non-compressible flow (liquid), the specific volume is essentially constant and generalized orifice equation can be reduced to the following expression

$$G = \sqrt{2g_c\rho(P_0 - P)} \tag{31}$$

Assumption

1. Specific volume = $(\frac{1}{\hat{V}_{mix}})$ = constant

27

Compressible fluid conditions can be characterized as either ideal gas or non-ideal gas conditions. Under ideal gas conditions, the relationship between pressure and volume is governed by the ideal gas equation and ,under isentropic conditions, the pressure and specific volume yields the following relationship

$$P\hat{V}^k = \text{constant} \tag{32}$$

where

$k = \text{Cp}^{\text{IG}} / \text{Cv}^{\text{IG}} = $ Ideal gas specific heat ratio

Cp $^{\text{IG}}$ is the ideal gas heat capacity at constant pressure

Cv $^{\text{IG}}$ is the ideal gas heat capacity at constant volume

The application of equation 30 and the ideal gas equation

$$\hat{V} = \frac{ZRT}{MwP} \tag{33}$$

where

Z is the Compressibility factor (1 for ideal gas)

Mw is the molecular weight of the vapor/gas

R is the universal gas constant

The ideal gas isentropic nozzle equation for ideal gas is simplified to the flowing expression.

$$G = P_1 \sqrt{\frac{M_w}{T_1 Z_1}} \left\{ 520 \sqrt{k \left(\frac{2}{k+1} \right)^{\frac{k+1}{k-1}}} \right\} \qquad (34)$$

The real gas isentropic nozzle equation is summarized as follows

$$G = \left(2gc \frac{Po}{\widehat{V}o} \right)^{1/2} \left(\frac{n}{n-1} \right)^{1/2} \left\{ \left(\frac{P}{Po} \right)^{\frac{2}{n}} - \left(\frac{P}{Po} \right)^{\frac{n+1}{n}} \right\}^{1/2} \qquad (35)$$

where

n is the isentropic expansion coefficient.

gc is the gravitational conversion factor

G is the mass flux through the nozzle

$\widehat{V}$ is the specific volume of the fluid

P is the pressure of the fluid

o represents conditions at the inlet of the nozzle

t represents conditions at the throat of the nozzle

The flow velocity through the nozzle and the downstream pressure of the relief valve determines the mass flux through the nozzle (see Figure 3.2). In general, the stagnant pressure (Po) should be higher than downstream pressure (P_1) conditions to enable a constant flow of vent gas through the orifice of the pressure relief valve. The flow rate through the orifice shall increase if the stagnant pressure (Po) remains fixed and downstream pressure P_1 decreases. Conversely, the flow rate through the orifice shall decrease at higher downstream pressure conditions up until the

29

pressures are the same (ie Po=P$_1$), at which point there will be no flow through the nozzle. However, when the downstream pressure is equal to the system critical pressure (i.e. P$_1$= Pc)
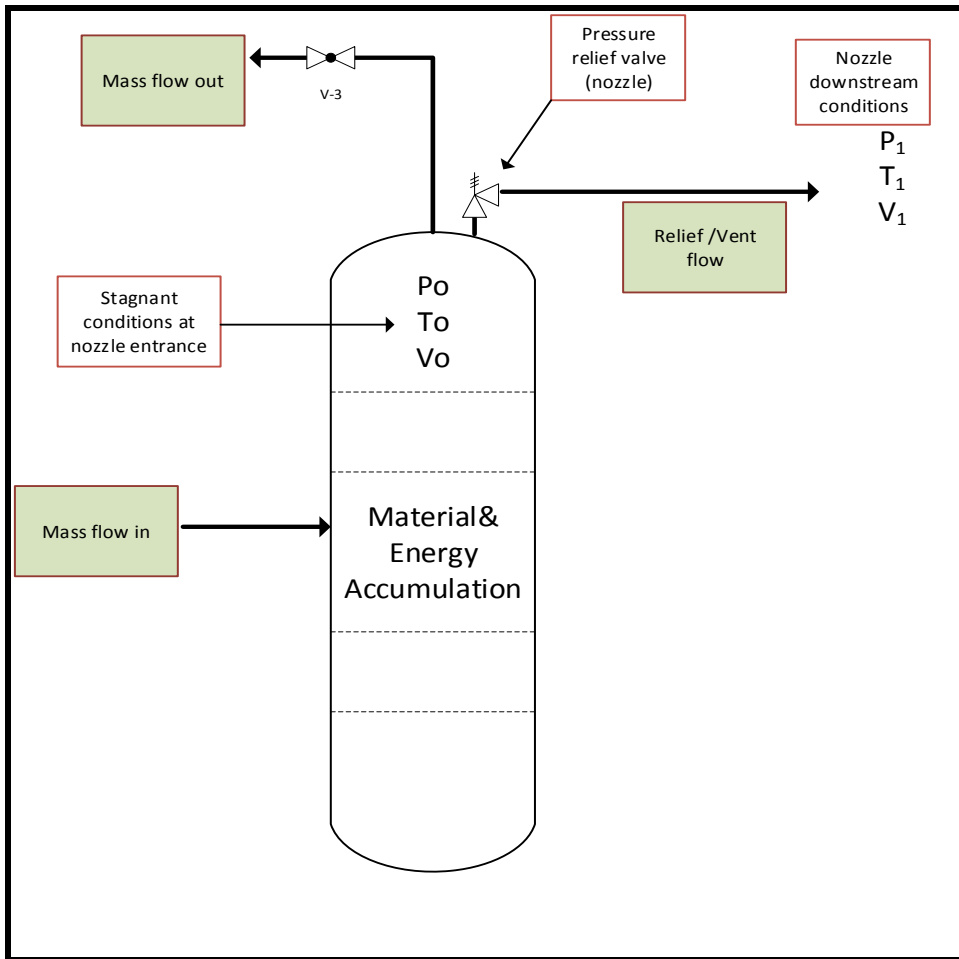
Figure 3.2: Pressure relief valve orifice upstream and downstream conditions.

choked flow conditions shall prevail. At choked flow conditions, the maximum velocity (sonic) is attained across the nozzle. At this point the only means of increasing the flow rate through the relief valve nozzle is to increase the stagnant pressure Po. Choked flow conditions can be verified according to equation 35-1.

$$\left(\frac{P_1}{Po}\right) \leq \left(\frac{P_c}{Po}\right) = \left(\frac{2}{n+1}\right)^{\frac{n}{n-1}} \tag{35-1}$$

If chocked flow conditions prevail, the mass flux through the nozzle can be calculated according the equation 35-2

$$Gc = \sqrt{n\frac{Po}{\widehat{V}o}\left(\frac{2}{n+1}\right)^{\frac{n+1}{n-1}}} \qquad (35\text{-}2)$$

where metric units are utilized

$$Gc = \sqrt{4633n\frac{Po}{\widehat{V}o}\left(\frac{2}{n+1}\right)^{\frac{n+1}{n-1}}} \qquad (35\text{-}3)$$

where imperial units are utilized

Equation 35 is a suitable expression for estimation the mass flux through an orifice for mildly non -ideal gases. The typical range of compressibility factors ranging between 0.8 and 1.1.

The relationship between pressure and specific volume over an isentropic path of expansion can be expressed according to equation 36, assuming constant isentropic expansion factor (n)

$$P\widehat{V}^n = P_0\,\widehat{V}_0^n \qquad (36)$$

where

n is the isentropic expansion fact

$$n = -\frac{V}{P}\left(\frac{dP}{dV}\right)_T\left(\frac{Cp}{Cv}\right) \qquad (37)$$

The application of equation 37 assumes a constant isentropic expansion factor. However, the isentropic expansion factor can be attained from an equation of state which is a function of pressure and specific volume. The isentropic co-efficient is assumed to be constant based on the expression on equation 37, which is not entirely correct. The changes in the value of the isentropic efficiency are assumed to be negligible with the upper and lower limits of pressure that are assessed.

3.2.1. Calculation of isentropic expansion factor

There are two methods that are commonly used to calculate the isentropic expansion factor. This includes an analytical method and a numerical method.

3.2.1.1.   Isentropic expansion factor: Analytical calculation method

By applying an equation of state to equation 37 an expression can be derived for the isentropic expansion factor. The equation of state selected in this case is the Redlich-Kwong equation of state (as an example).

$$P = \left(\frac{RT}{\hat{V}-b}\right) - \left(\frac{a}{\hat{V}(\hat{V}+b)T^{1/2}}\right)$$

where

$$a = 0.42748\left(\frac{R^2 T_c^{5/2}}{P_c}\right)$$

$$b = 0.08664\left(\frac{RT_c}{P_c}\right)$$

When the above expressions from equations 9, 10 and 11 are substituted into equation the general formal of the isothermal expansion factor (equation 37). The following outcome arises. (see equation 38)

$$n = \left(\frac{\hat{V}}{P}\right)\left[T\left(\frac{1}{Cv^{IG}}\right)\left(\frac{dP}{dT}\right)^2 - \left(\frac{dP}{d\hat{V}}\right)\right] \tag{38}$$

where

n = real gas isentropic expansion exponent

$\hat{V}$ = real gas molar specific volume equation

P = absolute pressure

The terms in equation 38 are derived by applying the required variable derivative to the Redlich Kwong equation of state (see equations 39-41)

$$\left(\frac{dP}{dT}\right)_{\hat{V}} = \left(\frac{R}{\hat{V}-b}\right) + \left(\frac{a}{\hat{V}*(\hat{V}-b)2T^{3/2}}\right) \tag{39}$$

$$Cv^{IG} = \left(\frac{R}{k-1}\right) + \left(\frac{3a\ln\left(1+\frac{b}{\hat{V}}\right)}{4bT^{\frac{3}{2}}}\right) \tag{40}$$

$$\left(\frac{dP}{d\hat{V}}\right)_T = RT\left(\frac{1}{\hat{V}-b}\right)^2 + \left(\frac{a(2\hat{V}+b)}{T(\hat{V}+b\hat{V})^{\frac{1}{2}}T^{1/2}}\right) \tag{41}$$

where

k = Ideal gas specific heat ratio

R = universal gas law constant

T = absolute Temperature

P = absolute pressure

Tc = critical temperature

Pc = critical pressure

The solution for the isentropic expansion co-efficient can be attained analytically using equations 38 through 41.

3.2.1.2.   Isentropic expansion factor: Process simulation method

The alternative approach is to utilize a process simulation engine such as Aspen Plus instead of the analytical method, that would require manual computation. The methodology entails setting up a flowsheet with three modules that include an inlet line, and expander and an outlet line. The isentropic efficiency for the expander shall be set at 75%. The objective of the flow scheme (Figure 3.3) is to enable the user to generate data points of pressure vs molar specific volume (P vs $\hat{V}$). Equation 36 can be converted to a linear expression in order to determine the value of the isentropic expansion factor (n).
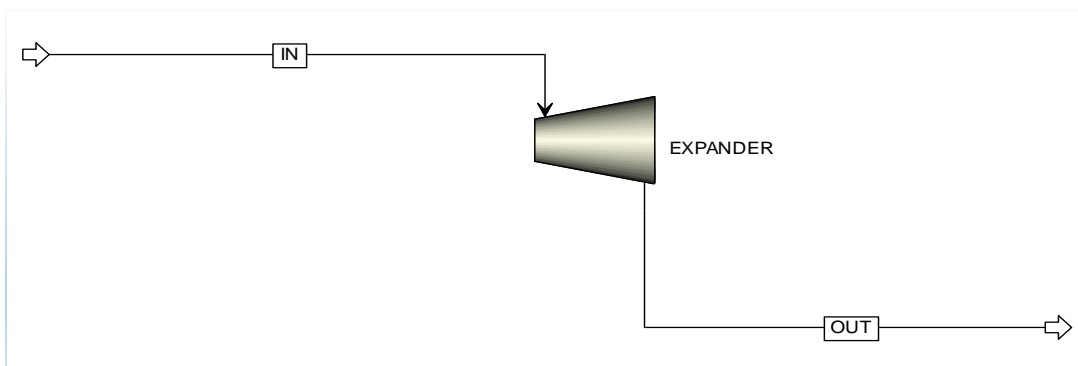
Figure 3.3: Aspen Plus isentropic expansion flow scheme

$$\ln\left(\frac{P}{P_o}\right) = n\ln\left(\frac{V_o}{V}\right) \tag{42}$$

The gradient of the straight-line curve generated by plotting the data according to equation 42. The gradient of the line shall be the isentropic expansion coefficient.
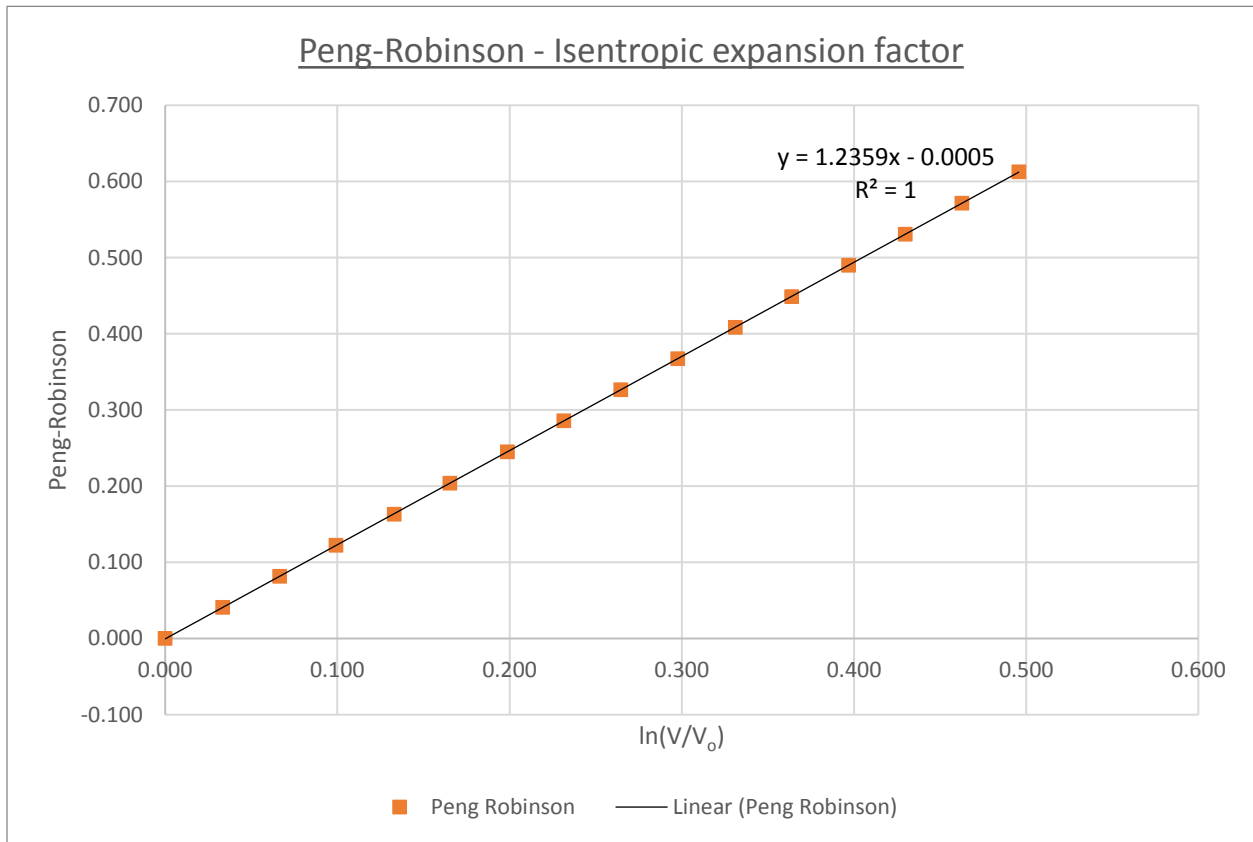
Figure 3.4: Isentropic expansion coefficient estimation (Peng-Robinson - EoS)
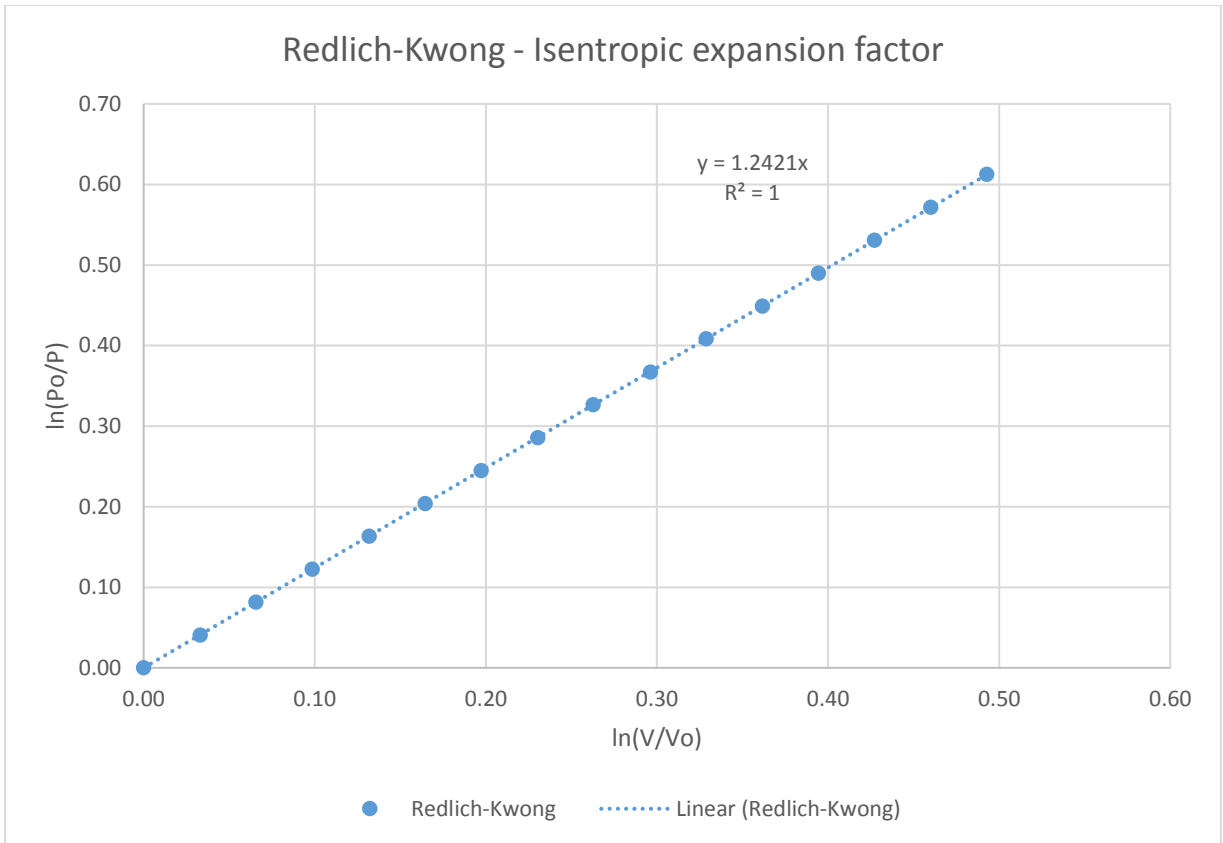
Figure 3.5 : Isentropic expansion coefficient estimation (Redlich-Kwong - EoS)
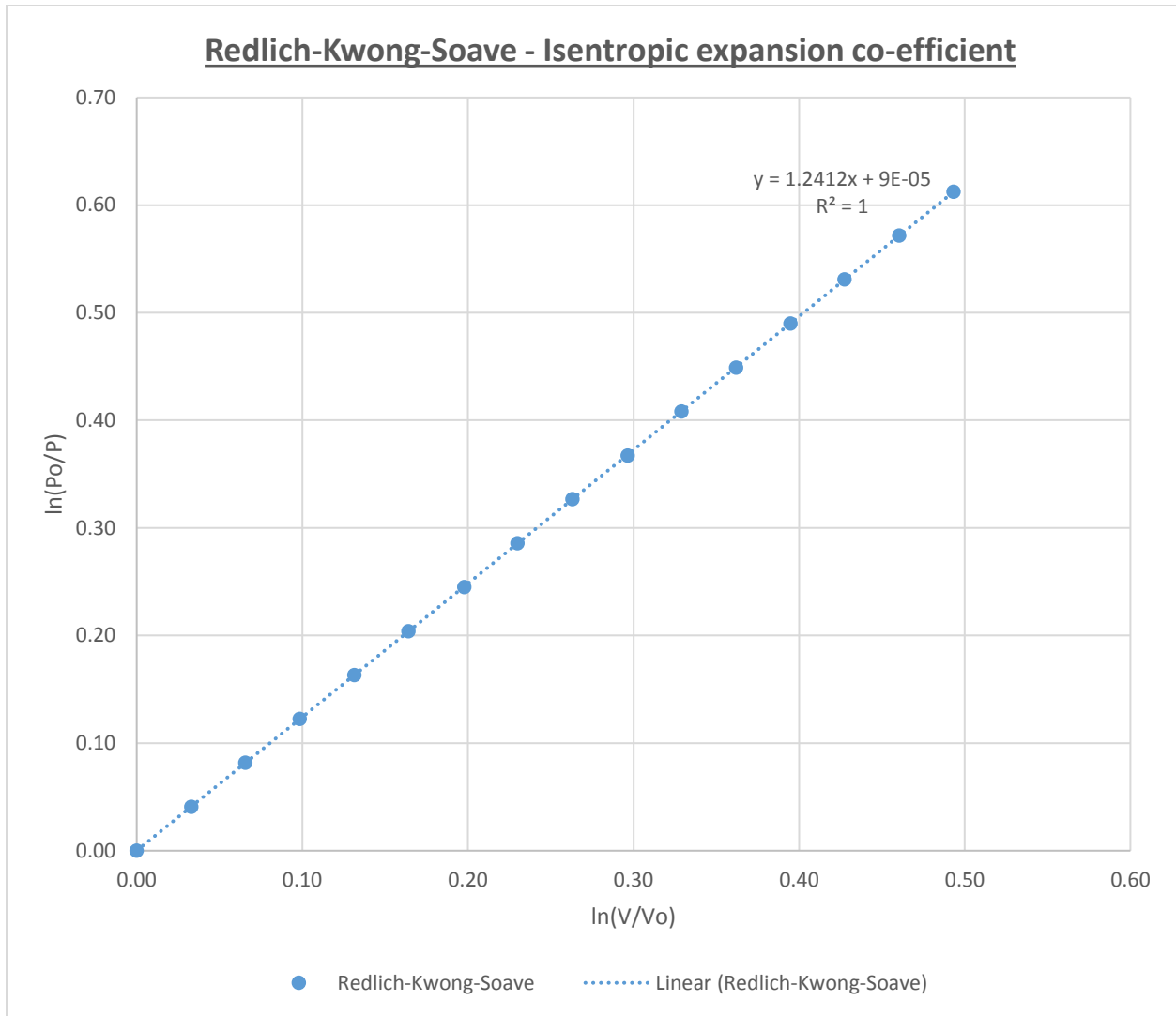
Figure 3.6 : Isentropic expansion coefficient estimation (Soave Redlich-Kwong - EoS)

Equation of State	Isentropic expansion Factor	Factor
Ideal Gas	1.254	$K = Cp^{IG}/Cv^{IG}$
Peng-Robinson	1.236	n
Redlich-Kwong	1.242	n
Redlich-Kwong Soave	1.241	n

Table 3.1: Equation of state isentropic expansion factors

The isentropic expansion factors and the heat capacity ratio were applied to equation 34 and 35 in order to determine the mass flux associated with each of the non-ideal equations of state and the ideal gas equation. The results are summarized on Table 3.1 of the non-ideal mass flux approximations

3.3. The calculation of the mass flux through the relief valve orifice.

3.3.1. Mass flux calculation: API simplified method

The simplified API mass flux calculation method involves a two-step process. The first step involves establishing whether the flow rate through the relief valve orifices is choked. This determination is crucial as it dictates the equations that shall be relevant to determine the mass flux through the orifice. The second step entails applying the isentropic expansion factor to either equation 35 (non-choked flow) or equation 35.2 (choked flow) to determine the mass flux through the pressure relief valve orifice. Based on the assessment of the Aspen plus simulation generated data, it was apparent that the relief conditions satisfied the choked flow conditions as prescribed in equation 35.1, the results are summarized in Table 3.2

Equation of State	Isentropic expansion factor	Pc/Po	P$_1$/Po	P$_1$ (psia)	Po (psia)	Comments
Ideal Gas	1.254	0.5543	0.5408	237.00	438.20	Pc/Po > P$_1$/Po Therefore flow is choked
Peng-Robinson	1.236	0.5576				
Redlich-Kwong	1.2421	0.5564				
Soave Redlich Kwong	1.2412	0.5566				

Table 3.2: Choked flow assessment

The subsequent mass flux estimations based on the simple API method (equations 35.2 and 35.3) are summarized in Table 3.3 below. The results indicate a significant percentage deviation of the mass flux calculated using the cubic equations of state, relative to the ideal gas equation of state. The relative percentage is in excess of 20% for each of the cubic equations of state whilst the relative difference between each of the cubic equations of state is less than 2%.

Equation of State	Isentropic expansion factor	gc lbm-ft/lbf.sec^2	Po (psia)	Po (lb/ft^2)	Vo (ft^3/lb)	Gc (lb/s.ft^2)	Gc (lb/hr.in^2)	Gc deviation from IG %
Ideal Gas	1.254	32.17	423.5	60984.0	0.62	1663.90	41597.51	-
Peng-Robinson	1.236	32.17	423.5	60984.0	0.6037	1671.00	41774.93	-0.43
Redlich-Kwong	1.2421	32.17	423.5	60984.0	0.6108	1664.28	41606.99	-0.02
Soave Redlich-Kwong	1.2412	32.17	423.5	60984.0	0.6088	1666.51	41662.80	-0.16

Table 3.3: API simple method mass flux calculation summary

3.3.2. Mass flux calculation: Direct integration method

The most accurate sizing method for non-ideal gases is the direct integration method. The method involves using a numerical technique such as the trapezoidal rule to quantify the integral of the specific volume between the bounds of the system static pressure and the relief system back pressure or the critical pressure. This is in order to quantify the mass flux as per equation 6. The lower limit of pressure (at which the specific volume integral is determined) is fixed by the maximum mass flux computation. If the flow is characterized as choked, the maximum mass flux shall be attained at a pressure that is higher than the system back pressure. For non-choked conditions, the maximum mass flux shall be coincident with the integral assessed pressure

$$G = \frac{1}{\hat{V}}\left[-2g_c \sum 0.5(\hat{V}_i + \hat{V}_{i+1})(P_{i+1} - P_i)\right]^{1/2} \tag{43}$$

where

I = Integrand = $0.5(\hat{V}_i + \hat{V}_{i+1})(P_{i+1} - P_i)$

S = Summation = $\sum 0.5(\hat{V}_i + \hat{V}_{i+1})(P_{i+1} - P_i)$

The computation of the mass flux involves evaluating the specific volume at different pressure values between the static pressure and the relief pressure. The computation of the mass flux can be executed in a tabulated format that indicates the mass flux at every pressure increment between the static pressure and the relief pressure. The nature of the flow characteristics can be deduced based on the trend in the mass flux values at each corresponding pressure increment. For critical

(choked) flow conditions, the integration (mass flux) shall reach a maximum value, which will coincide with the point at which the critical pressure (Pc) has been reached.

A summary of the mass flux integration for each of the selected property method is presented in Tables 3.4-3.7 below

Pressure (Psia)	Temperature oF	Mass Quality /Vapor fraction	Density lb/ft3	Integrand	Summation (ft2/s2)	Mass flux (lb/h/in2)
438.2	542.5	1	1.398	0	0	0
420.7	534.9	1	1.352	-59060.0	-59060.0	11620.0
403.8	527.4	1	1.308	-58610.0	-117700.0	15870.0
387.7	519.9	1	1.266	-58160.0	-175800.0	18760.0
372.2	512.5	1	1.224	-57710.0	-233500.0	20920.0
357.3	505.1	1	1.185	-57260.0	-290800.0	22580.0
343	497.7	1	1.146	-56820.0	-347600.0	23890.0
329.3	490.4	1	1.109	-56380.0	-404000.0	24920.0
316.1	483.1	1	1.073	-55950.0	-459900.0	25720.0
303.5	475.8	1	1.038	-55510.0	-515500.0	26350.0
291.3	468.6	1	1.004	-55080.0	-570500.0	26820.0
279.7	461.4	1	0.9716	-54650.0	-625200.0	27160.0
268.5	454.2	1	0.9401	-54220.0	-679400.0	27400.0
257.7	447.1	1	0.9096	-53800.0	-733200.0	27540.0
247.4	440	1	0.8801	-53380.0	-786600.0	27600.0
237.5	433	1	0.8516	-52960.0	-839600.0	27590.0

Table 3.4: Mass flux integration Peng-Robinson property method

Pressure (Psia)	Temperature oF	Mass Quality /Vapor fraction	Density lb/ft3	Integrand	Summation (ft2/s2)	Mass flux (lb/h/in2)
438.20	542.30	1.00	1.39	0.00	0.00	0.00
420.70	534.80	1.00	1.34	-59610.00	-59610.00	11570.00
403.80	527.30	1.00	1.30	-59140.00	-118700.00	15800.00
387.70	519.90	1.00	1.26	-58670.00	-177400.00	18680.00
372.20	512.50	1.00	1.21	-58210.00	-235600.00	20840.00
357.30	505.10	1.00	1.18	-57740.00	-293400.00	22500.00
343.00	497.80	1.00	1.14	-57290.00	-350700.00	23800.00
329.30	490.50	1.00	1.10	-56830.00	-407500.00	24830.00
316.10	483.20	1.00	1.07	-56380.00	-463900.00	25630.00
303.50	476.00	1.00	1.03	-55930.00	-519800.00	26260.00
291.30	468.80	1.00	1.00	-55490.00	-575300.00	26730.00
279.70	461.60	1.00	0.96	-55050.00	-630300.00	27080.00
268.50	454.40	1.00	0.93	-54610.00	-684900.00	27320.00
257.70	447.30	1.00	0.90	-54170.00	-739100.00	27460.00
247.40	440.30	1.00	0.87	-53740.00	-792800.00	27520.00
237.50	433.20	1.00	0.85	-53310.00	-846100.00	27520.00

Table 3.5: Mass flux integration Redlich-Kwong property method

Pressure (Psia)	Temperature oF	Mass Quality /Vapor fraction	Density lb/ft3	Integrand	Summation (ft2/s2)	Mass flux (lb/h/in2)
438.20	542.40	1.00	1.388	0.00	0.00	0.00
420.70	534.90	1.00	1.343	-59450.00	-59450.00	11580.00
403.80	527.40	1.00	1.300	-58990.00	-118400.00	15820.00
387.70	520.00	1.00	1.258	-58520.00	-177000.00	18710.00
372.20	512.50	1.00	1.217	-58060.00	-235000.00	20860.00
357.30	505.20	1.00	1.178	-57610.00	-292600.00	22520.00
343.00	497.80	1.00	1.139	-57150.00	-349800.00	23830.00
329.30	490.50	1.00	1.103	-56700.00	-406500.00	24850.00
316.10	483.20	1.00	1.067	-56260.00	-462700.00	25660.00
303.50	476.00	1.00	1.032	-55810.00	-518600.00	26280.00
291.30	468.70	1.00	0.999	-55370.00	-573900.00	26760.00
279.70	461.60	1.00	0.967	-54930.00	-628900.00	27100.00
268.50	454.40	1.00	0.935	-54500.00	-683400.00	27340.00
257.70	447.30	1.00	0.905	-54070.00	-737400.00	27480.00
247.40	440.20	1.00	0.876	-53640.00	-791100.00	27540.00
237.50	433.20	1.00	0.848	-53210.00	-844300.00	27540.00

Table 3.6: Mass flux integration Soave Redlich-Kwong property method

Pressure (psia)	Temperature oF	Mass Quality /Vapor fraction	Density lb/ft3	Integrand	Summation (ft2/s2)	Mass flux (lb/h/in2)
438.2	540.8	1	1.389	0.00	0.00	0.00
420.7	533.5	1	1.343	-59460.00	-59460.00	11400.00
403.8	526.2	1	1.299	-59020.00	-118500.00	15560.00
387.7	518.9	1	1.256	-58590.00	-177100.00	18390.00
372.2	511.6	1	1.215	-58160.00	-235200.00	20500.00
357.3	504.4	1	1.175	-57720.00	-293000.00	22130.00
343	497.2	1	1.136	-57290.00	-350200.00	23400.00
329.3	490.1	1	1.099	-56870.00	-407100.00	24410.00
316.1	482.9	1	1.063	-56440.00	-463600.00	25190.00
303.5	475.8	1	1.028	-56010.00	-519600.00	25800.00
291.3	468.7	1	0.9948	-55590.00	-575200.00	26250.00
279.7	461.7	1	0.9624	-55170.00	-630300.00	26590.00
268.5	454.7	1	0.9309	-54750.00	-685100.00	26810.00
257.7	447.7	1	0.9006	-54330.00	-739400.00	26950.00
247.4	440.7	1	0.8712	-53920.00	-793300.00	27000.00
237.5	433.8	1	0.8429	-53500.00	-846800.00	26990.00

Table 3.7: Mass flux integration ideal gas property method

The results in tables 3.4-3.7 indicate that the maximum mass flux is reached in the vicinity of the system operating pressure (237-247 psia). This confirms that choked flow conditions prevail. The highest mass flux appears to vary according to the property method selected. A measure of the extent of mass flux departure relative to the ideal gas conditions, is summarized in Table 3.8 for each property method and the pressure relief valve orifice sizing algorithm.

Equation of State	Isentropic expansion factor n	ADI Method		API simplified method		ADI method vs API method
		Gc (lb/hr.in2)	Gc deviation from IG %	Gc (lb/hr.in2)	Gc deviation from IG %	Gc Relative Difference %
Ideal Gas	1.254	27000.00	-	41597.51	-	54.06
Peng Robinson	1.236	27600.00	2.22	38562.97	-7.29	39.72
Redlich Kwong	1.2421	27520.00	1.93	38914.62	-6.45	41.40
Redlich Kwong Soave	1.2412	27540.00	2.00	38944.27	-6.38	41.41

Table 3.8: Mass flux deviation relative to ideal gas property method

Table 3.8 suggests a higher accuracy associated with the ADI method for sizing the relief valve orifice. The relative deviation in the mass flux estimation for each cubic equation of state is approximately four times greater (relative to the ideal gas equation of state) when applying the simplified API method formula in comparison to the direct integration method. This may be attributed to the fact that the API simplified method is only suitable for mildly non ideal gases ($0.8 < Z < 1.1$) and ethylene oxide is highly non ideal and the system compressibility factor is greater than 1.1.

Chapter 4 - Non ideal relief load calculations

4.1. Certified mass flux calculation

The mass flux estimated from equations 35 and 43 is a theoretical mass flux. In order to account for the actual conditions across the orifice and the design of the pressure relief valve, several correction factors are applied to the ideal mass flux. The factors include:

Kd: Coefficient of Discharge (experimentally determined by manufacturer)

Kc: Combination factor

Kb: Back pressure correction factor

Kv: viscosity correction factor

The coefficient of discharge is determined experimentally, by the valve manufacturer, whilst the combination factor accounts for the flow path through the relief valve and it adjusts the flow for a rupture disk that is installed in parallel with a relief valve. The back-pressure correction factor is used to adjust the flow for balanced safety relief valves with excessive back pressure. The viscosity correction (Kv) factor is applied at low Reynolds numbers to adjust for non-inviscid flow conditions, under which the coefficient of discharge (Kd) is determined experimentally. Typically, the coefficient of discharge is measured at high Reynolds numbers in the order of 10000.

$$K_v = \left[0.9935 + 2.787/N_{Re}^{0.5} + 342.75/N_{Re}^{1.5}\right)\,\right]^{-1} \tag{44}$$

where:

N_{Re} is the Reynolds number.

After applying the abovementioned correction factors, the actual mass flux can be estimated based on equation 45

$$G_{actual} = K_d K_c K_v K_b G^{Ideal\ Nozzle} \tag{45}$$

The relationship between the Pressure relief valve orifice cross sectional area and the actual mass flux is defined according to equation 46

$$W_{actual} = A_{device} G_{actual} \tag{46}$$

where,

W_{actual} is the relief mass flow rate

A_{device} the cross-sectional area of the Pressure relief valve

The design relief mass flow rate was set at an arbitrary value of 10,000 lb/hr. The stream conditions at relief pressure and temperature were estimated as full vapor. Therefore, the required relief valve area could be estimated from equation 46. The significant input required to calculate the required relief device cross sectional area, can be determined upon calculation of the actual mass flux (G_{actual}) utilizing equation 45.

The assumptions applied for the calculation are based on relief conditions of the Ethylene oxide reactor discharge stream.

Co-efficient	Value	Comments
Kd	0.85	Generic API factors for vapor streams. In practice this is 0.9Kd
Kc	1	PRV is the solitary device with no rupture disk beneath it
Kb	1	Downstream piping is designed within the above backpressure criteria, no backpressure capacity correction
Kv	1	The viscosity factor is unitary. Low Reynolds number conditions

Table 4.1: Summary of relief valve sizing correction factors

The actual mass flux and required orifice area for the different thermodynamic packages can be calculated based on the abovementioned correction factors.

	ADI method		API Simplified Method	
Equation of State	Gc (lb/hr/in²)	Area in²	Gc (lb/hr/in²)	Area in²
Ideal Gas	27000.00	0.436	41597.51	0.283
Peng Robinson	27600.00	0.426	38562.97	0.305
Redlich Kwong	27520.00	0.427	38914.62	0.302
Redlich Kwong Soave	27540.00	0.427	38944.27	0.302

Table 4.2: Summary of relief valve sizes based on EoS and sizing method

The relief valve orifice sizing method and the equation of state influence the determination of the orifice size in an opposing manner. The result suggests a diverging relationship between the two factors. The direct integration method yields a lower mass flux (and subsequently larger orifice area) for the ideal gas equation of state estimation. The converse relationship is observed for each of the cubic equations of state, whereby the direct integration method estimates a higher mass flux (and a subsequently smaller orifice area). The other significant observation is the relatively close approximation between the Redlich-Kwong and Redlich-Kwong Soave equations of state in comparison to the Peng-Robinson equation of state.

Relief Valve Orifice Size		
Letter	**Bore Dimensions**	
	in²	**cm²**
D	0.11	0.71
E	0.196	1.26
F	0.307	1.98
G	0.503	3.24
H	0.785	5.06
J	1.287	8.3
K	1.838	11.85
L	2.853	18.4
M	3.6	23.23
N	4.34	28
P	6.38	41.16
Q	11.05	71.29
R	16	103.22
T	26	167.74

Table 4.3: API standard relief valve orifice sizes

Equation of State	G actual	Mass Flow	Required area	API orifice size	
	lb/h/in²	**lb/hr**	**in²**	**Letter**	**in²**
Ideal gas	22950.00	10000	0.436	G	0.503
Peng Robinson	23460.00	10000	0.426	G	0.503
Redlich Kwong	23392.00	10000	0.427	G	0.503
Redlich Kwong Soave	23409.00	10000	0.427	G	0.503

Table 4.4: Summary of direct integration method relief valve sizes for different EoS

The direct integration method is generally a more accurate calculation method because its application is not limited to uses for fluid conditions that are characterized by a narrow range of

compressibility factors (0.8<Z<1.1). Therefore, a more accurate comparison of the relief valve orifice sizes would arise from the direct integration methods (see Table 4.4). A summary of all PRV parameters associated with each equation of state is highlighted in Table 4.5

Equation of State	Ideal Gas	Peng-Robinson	Redlich Kwong	Redlich-Kwong Soave
Calculated Orifice [in²]	0.436	0.426	0.427	0.427
Selected Orifice [in²]	0.503 (G)	0.503 (G)	0.503 (G)	0.503 (G)
Rated capacity [lb/hr]	11730.0	11800.0	11580.0	11780.0
Capacity Used[%]	85.27	84.76	86.32	84.92
Orifice Designation	1.5G3	1.5 G3	1.5G3	1.5G3
In/out Flanges	300X150	300X150	300X150	300X150
Discharge Coefficient (Kd)	0.85	0.85	0.85	0.85

Table 4.5 : Summary of relief valve size estimation based on the equation of state

Chapter 5 - Literature review on cubic equation of state accuracy

The conventional practice for determining the accuracy of a cubic equation of state, involves a comparison of thermodynamic properties predicted using cubic equations of state against real P,V,T data. However, there was no P,V,T data generated for the system under review for this masters report. The literature review was conducted to investigate the performance of the different cubic equations of state for similar systems where experimental data was available. The ultimate objective is to determine whether a correlation could be drawn between the deviation from ideality and the extent of relative error for systems that comprise components with a similar molecular structure. The assessment shall include a comparison of the relative deviation of thermodynamic properties for polar and non-polar components from the work done by Zabaloy and Vera [22], for each cubic equation of state. The extent of relative deviation for each cubic equation of state shall be ranked and evaluated against a similar ranking of the deviation from the PRV mass flux prediction using ideal equations of state.

The accuracy of the Peng-Robinson equation of state was compared with the Van der Waals and the Redlich-Kwong cubic equations of state by Zabaloy and Vera. The test involved comparisons of the cubic equation of state using two different forms of the alpha (α) function and experimental data derived from the DIPPR data base [23].

The forms of the alpha function were a modification of the original forms of the Peng-Robinson and Redlich-Kwong cubic equations of state, as specified in equations 16 and 13 respectively. The alpha (α) function forms include the PSRV2 and the ZPVR form. The PSRV2 form is based on a dependence in terms of the reduced temperature and the acentric factor, whilst retaining the same alpha (α) general function. The modifications included essentially a change to the k parameter equation (such as in equation 18).

$$k = ko + \ [\ k_1 + k_2(k_3 - T_r)(1 - T_r^{0.5})](0.7 - T_r) \tag{47}$$

$$ko = 0.37889 + 1.489716\omega - 0.17132\omega^2 + 0.01965\,\omega^3 \tag{48}$$

where

k_1, k_2, k_3 are characteristic parameters for each compound

The PRSV2 form of alpha is attained by setting a value of $k_2, = 0$, for equation 47.

The relationships between the k parameters and the acentric factor is simplified significantly when the experimental data is reviewed at a specific reduced temperature of 0.7 (Tr =0.7). At this condition, the universal relationship expressed in equation 14-4 is satisfied. Another form of equation 14-4 is highlighted as equation 49.

$$\omega = -log_{10}(P_r^{sat}) - 1 \tag{49}$$

where

$$P_r^{sat} = \frac{P^{sat}}{Pc}$$

The ZVPR alpha function arose from modification to the Peng-Robinson equation of state. The modification is based on a different functional form of the alpha (α) general function.

$$\alpha = T_r F[\ P_r / T_r] \tag{50}$$

where

F is a universal function that is dependent on the EoS chosen

By incorporating the universal acentric factor (equation 49) with equation 50 and applying a polynomial expansion. A simplified expression of alpha is achieved that is in terms of the reduced temperature for the difference in the heat capacity of the saturated phases.

$$\alpha = 1 + C_1 T_r ln T_r +\ C_2 (T_r - 1) + C_3 (T_r^2 - 1) \tag{51}$$

where

C_1, C_2,C_3 are determined from three experimental points

The values of C_1,C_2, C_3 are determined at specific temperatures where equation 50 reproduces an identical value of the experimental vapor pressure. The data points include conditions at Tr =0.7, which enabled the experimental vapor pressure information to force the equation of state to reproduce the exact experimental value of w at Tr =0.7.

The evaluation of each cubic equation of state was based on a combination of polar, non-polar and associating compound molecules namely; methane, water, di iso propyl ether, water, ammonia, n-octane, sulfur dioxide., n-nitrotoluene. The results provided a comparison of the calculated saturated molar volumes, when the pure compound vapor pressure is matched according to the algebraic form of each cubic equation of state at the corresponding temperature

Table 5.1 highlights the comparison in relative errors of thermodynamic properties (with respect to experimental data) between the Redlich-Kwong and Peng Robison's equations of state. The assessment is based on the PSRV2 form of the alpha function. Furthermore, the predicted thermodynamic properties are estimated using an approach whereby each equation state form is forced to exactly reproduced the experimental vapor pressures at the triple point, normal boiling point and at Tr =0.7.

		Peng-Robinson			Redlich Kwong		
Compound	Polarity	ΔV-L , %	ΔV-V, %	ΔP-S, %	ΔV-L , %	ΔV-V, %	ΔP-S, %
Methane	non polar	8.3 (15.7)	1.6 (8.1)	0.17 (0.46)	5.6 (26.4)	0.9 (7.8)	0.21 (0.53)
n-octane	non polar	6.8 (32.3)	0.80 (14.1)	0.18 (0.49)	20.4 (44.6)	0.9 (23.4)	0.51 (1.19)
Diisopropyl ether	dipole moment	4.3 (23.5)	2.8 (10.2)	2.27 (7.20)	11.3 (34.9)	3.5 (19.2)	2.02 (6.44)
water	polar	25.7 (54.2)	2.7 (27.5)	0.08 (0.32)	41.7 (68.9)	3.6 (37.9)	0.10 (0.30)

Table 5.1: Average relative deviation (%) in vapor pressure, saturated liquid and vapor volumes based on PRSV2 approach for α

Table 5.2 highlights a similar comparison in relative errors of thermodynamic properties (with respect to experimental data) between the Redlich-Kwong and Peng Robison's equations of state. The assessment is based on the ZVPR form of the alpha function. Furthermore, the predicted thermodynamic properties are estimated using a similar approach the PRSV2 approach whereby each equation state form is forced to exactly reproduced the experimental vapor pressures at the triple point, normal boiling point and at Tr =0.7.

Some simplifying assumptions were made, the most significant being a fixed value of the k_3 parameter for all the cubic equations of state for the PRSV2 case. In spite of this, the approach that was applied was deemed to be fair an acceptable due to the following reasons

- The experimental database considered was the same
- The method used for determining the parameters k_0, k_1, k_2 and the C_1, C_2, C_3 constants gives a unique set of values for each EoS and each compound
- The same points were used to determine the coefficients of the alpha functions

Compound	Polarity	Peng-Robinson			Redlich Kwong		
		ΔV-L , %	ΔV-V, %	ΔP-S, %	ΔV-L , %	ΔV-V, %	ΔP-S, %
Methane	non polar	8.3 (15.7)	1.6 (8.0)	0.13 (0.34)	5.5 (26.3)	0.9 (7.8)	0.13 (0.33)
n-octane	non polar	6.7 (32.3)	1.0 (14.2)	0.29 (1.08)	20.3 (44.5)	1.2 (23.4)	0.20 (0.71)
Diisopropyl ether	dipole moment	4.5 (24.0)	1.2 (10.1)	0.72 (2.71)	11.6 (35.4)	1.8 (19.0)	0.60 (2.32)
water	polar	25.7 (54.1)	2.7 (27.5)	0.12 (0.40)	41.7 (68.8)	3.8 (37.9)	0.06 (0.24)

Table 5.2: Average relative deviation (%) in vapor pressure, saturated liquid and vapor volumes based on ZVPR approach for α

The most important factors summarized in Table 5.1 and Table 5.2, that are relevant to the sizing of PRVs include

- The average absolute relative deviation for saturated vapor volumes (ΔV-V)

- The average absolute relative deviation for saturated vapor pressure (ΔP-S)

The lowest average absolute relative deviation for either saturated vapor volumes or vapor pressure, represents the most accurate prediction of the respective parameters.

For polar compounds, the results suggest that the Peng Robison EoS demonstrates the lowest average absolute relative deviation for saturated vapor volume (ΔV-V) prediction for both alpha (α) functions (PRSV2 and ZPVR). Furthermore, Peng Robison EoS shows the lowest average absolute relative deviation for saturated vapor pressure (ΔP-S) prediction for the PRSV2 alpha (α) function.

The non-polar components showed a greater degree of inconsistency (relative to polar components).The lowest average absolute relative deviation for saturated vapor volume (ΔV-V) prediction differs for both non-polar components. Both components show good agreement with different equations of state. Peng Robison and Redlich-Kwong demonstrated the best fit for octane and methane respectively and the observation is consistent for both alpha (α) functions (ZPVR and PRSV2).

The lowest average absolute relative deviation for saturated vapor pressure (ΔP-S) prediction differed for both non-polar components. For methane, the basis of the difference was the alpha (α) function since Peng Robison and Redlich-Kwong EoS both demonstrated the lowest average absolute relative deviation for saturated vapor Pressure (ΔP-S) prediction, only for the ZPVR alpha (α) function.

For octane, the Redlich-Kwong EoS demonstrated the lowest average absolute relative deviation for saturated vapor pressure (ΔP-S) prediction only for the ZPVR alpha (α) function

Chapter 6 - Conclusion

The intent of the study was to review two factors that influence the size of pressure relief valves in high pressure, non-ideal chemical processes: the two factors included the equation of state and the pressure relief valve orifice dimension calculation methods. The system that was chosen to explore this was a gas a phase mixture from an ethylene oxide synthesis reactor.

The selection of an appropriate equation of state was the first factor to be evaluated. The selection criteria was influenced primarily by the molecular structure of the stream components. There was a mixture of polar and non-polar components (i.e. ethylene oxide, carbon dioxide, etc.) However, the components with the strongest interaction was presumed to be ethylene oxide, due to the presence of several types of interactions (dipole-dipole and London) and the exhibited high propensity of the oxarine molecules to dissociate. The conditions of the stream included a high pressure (above 10 bar) yielding non ideal conditions where the use of the ideal fluid assumptions would yield errors in the prediction of compound properties such as vapor pressure and saturated liquid volumes. The impact of EoS selection was assessed for three cubic equations of state and their departure from ideality was measured against the ideal gas assumptions (ideal gas equation and Daltons law etc.). The measure of deviation was the mass flux across the pressure relief valve, which was calculated as a function of the specific volume at different pressure increments between the system operating pressure and the relief pressure. The computation of the mass flux was therefore dependent on the EoS selected to predict the pressure, temperature and volume of the mixture.

The results confirmed that most of the cubic equations of state exhibited a large departure form ideal gas assumption (in excess of 6 %) the largest deviation noticed was for the Peng-Robinson equation of state. However, the Redlich-Kwong and Redlich-Kwong Soave were less than 2% apart from the Peng-Robinson equation of state and were less than 0.5% apart in terms of the relative difference from each other.

The Peng-Robinson equation of state suggested a greater indication of real gas approximation. This assertion is supported by the following observations.

- Peng-Robinson was the only cubic equation of state that has non-zero values for all parameters included in the general form of the equation see Table 2.2
- Peng-Robinson has been modified by many authors leading to a greater level of accuracy at predicting physical properties of compounds
- The comparison of compounds of polar, non-polar and associative structure from literature reviews (similar to the compounds in this study) demonstrate the least error in the prediction of molar volumes and saturation pressure for polar and non-polar compounds, when applying the Peng-Robinson EoS. The observation was consistent for different EoS parameters

The second factor that influenced the accuracy of the prediction of the pressure relief valve orifice size was the selected method for estimating the mass flux through the orifice. Two methods were compared, API simplified method and the direct integration method. The API simplified method is an empirical method that is dependent on the isentropic co-efficient of expansion factor. The significant shortcoming with this method is the narrow range of compressibility factors ($0.8 < Z < 1.1$) within which the method is applicable. This renders the method suitable only for systems that deviate moderately from ideal gas conditions. The direct integration method is more rigorous and requires the direct input of molar volume and corresponding pressure values based on the selected equation of state.

The results indicated a lower relative deviation in the mass flux calculation for all equations of state (in comparison to the API simplified method). The observation suggests that direct integration method is more consistent especially when the system contains highly non ideal polar molecules. Therefore, the appropriate method for determining the correct pressure relief valve orifice size for a similar system should include the following steps:

- Selection of the Peng-Robinson equation of state to determine physical properties
- Applying the direct integration method to determine the theoretical / ideal orifice mass flux.

Furthermore, the cubic equations of state evaluated do not exhibit a significant difference in the mass flux prediction. The difference is relatively insignificant form industrial process design and it would not lead to an inappropriate selection of a PRV. This is because commercial relief valves are offered in standard sizes (API standard orifice sizes in Table 4.3) that encompass a significant margin of capacity. As a result, in some instances the inaccuracy associated with using the API simplified method vs the direct integration method would yield no difference in the selection of the pressure relief valve size. The results on Table 4.2 indicate that this outcome was observed for the ethylene oxide system that was reviewed in this study. The result confirmed that the relief valve would have been undersized, however, if ideal gas conditions were assumed and the API simplified method was applied. This scenario would have yielded a size F orifice for the pressure relief valve. Such a pressure relief valve selection would have compromised the over pressure protection capacity of the system.

References

1. American Petroleum Institute Standards. API-520, Part 2, (2015) Sizing, Selection, and Installation of Pressure-relieving devices -Part II, Installation, 6TH Edition

2. American Society of Mechanical Engineers, ASME Section VIII. Div1 (2019), BPVC Section VIII-Rules for Construction of Pressure Vessels Division 1, UV

3. American Institute of Chemical Engineers. Center for Chemical Process Safety, CCPS (Center for Chemical Process Safety). (2017)., Guidelines for Pressure relief and effluent handling systems, (2), pp 285-299

4. EO/EG (Ethylene Oxide/Ethylene Glycol). (n.d.). Retrieved from https://www.toyo-eng.com/jp/en/products/petrochmical/eo/

5. Lou, Helen H, Chandrasekaran, Jayachandran; Smith, Rebecca A (2006). Large-scale dynamic simulation for security assessment of an ethylene oxide manufacturing process, Computers and Chemical Engineering, Vol.30(6), pp.1102-1118

6. Prihatin, T., Shuhaimi M, Abdul Mutalib, M. I., and Bustan, M.D. (2013). Synthesis of Optimum Water Polygeneration System in Ethylene Glycol Production, Industrial and Engineering Chemistry Research, Vol.52, pp.7069-7072

7. Crusius, J.P., Hellmann, R., Hassel, E., and Bich E. (2014). Intermolecular potential energy surface and thermophysical properties of ethylene oxide. The Journal of Chemical Physics. 141, pp 164322-2 - 164322-3

8. Traven VF (2004). Organic chemistry: textbook for schools. 2 ECC "Academkniga".
 pp. 102–106. ISBN 5-94628-172-0.

9. Hou, V. (n.d.). Guidelines for Choosing a Property Method Guidelines for Choosing a Property Method for Polar Non-Electrolyte Systems Guidelines for Choosing an Activity Coefficient Property Method. Retrieved from https://www.academia.edu/7721418/Guidelines_for_Choosing_a_Property_Method_Guidelines_for_Choosing_a_Property_Method_for_Polar_Non-Electrolyte_Systems_Guidelines_for_Choosing_an_Activity_Coefficient_Property_Method

10.   Georges, M. A., Gianetto, A., Levin, M., Fisher, H.G., Chippett, S., Singh S.K., Chipman., P.I., (2001) Kinetics of the reactions of ethylene oxide with water and ethylene glycols., Process Safety Progress, Vol.20(4), pp.231-246

11.   Sandler, S.I., (1940). Chemical, biochemical, and engineering thermodynamics, (4th edition),Wiley pp.190-198

12.   Silbey, R. J., Alberty, R. A., Bawendi, M.G., (2004). Physical Chemistry (4th ed.). Wiley. ISBN 978-0471215042.

13.   Prausnitz J.M., Lichtenthaler., Azevedo.,(1986) Molecular thermodynamics of fluid-phase equilibria (2nd Edition), Englewood Cliffs, N.J. : Prentice-Hall, pp 49-55

14.   Jaubert, J. N., Privat R., (2010) Relationship between the binary interaction parameters (kij) of the Peng-Robinson and those of the Soave – Redlich-Kwong equations of state; Application to the definitions of the PR2SRK model. Fluid Phase Equilibria Vol (295), pp 29-32

15.   Lopez-Echeverry J.S., Reif-Acherman S., Araujo-Lopez, E., (2017) Peng-Robinson equation of state: 40 years through cubics., Fluid Phase Equilibria Vol (447), pp 41-44

16.   Péneloux, A., E. Rauzy, E., Fréze, R., (1982), A consistent correction for Redlich-Kwong-Soave volumes., Fluid Phase Equilibria, Vol 8(1), pp. 7-23,

17.   Wei, Y.S., Sadus R.J., (2000)., Equations of state for the calculation of fluid-phase equilibria., AIChE Journal., Vol 46(1) pp. 169-196,

18.   Sandler S.I., (1994)., Models for Thermodynamic and Phase Equilibria Calculations: Marcel Dekker Inc., pp 363-506

19.   Perez, A.G.; Coquelet, C.; Paricaud, P. ; Chapoy, A., (2017)., Comparative study of vapor-liquid equilibrium density modelling of mixtures related to carbon capture and storage with the SRK, PR, PC-SAFT and SAFT-VR Mie equations of state for industrial uses, Fluid Phase Equilibria, Vol.440, pp.19-35

20.   Michelsen M.L., Mollerup J.M., (2004) Thermodynamic Models: Fundamentals and Computational Aspects (2nd ed.)

21.   Younglove.. B., Ely. J., (1987)., Thermophysical Properties of Fluid II. Methane, Ethane, Propane, Isobutane and Normal butane., Journal of Physical and Chemical Reference Data, (16)., pp. 557-797,

22.   Zabaloy S.M., Vera J.H., (1989)., The Peng-Robinson Sequel. An Analysis of the Particulars of the Second and Third Generation., Journal of Industrial and Engineering Chemistry , (37)., pp.1591-1597,

23.   Daubert, T.E. and Danner, R.P. (1989) Physical and Thermodynamic Properties of Pure Chemicals (Data Compilation). Hemisphere Publishing Corporation, New York.

Appendix A - Isentropic expansion data

P-psia	P - lb/ft²	Density lb/ft³	Po/P	ln(Po/P)	V/Vo	ln(V/Vo)
438.200	63100.800	1.398	1.000	0.000	1.000	0.000
420.700	60580.800	1.352	1.042	0.041	1.034	0.033
403.800	58147.200	1.308	1.085	0.082	1.069	0.067
387.700	55828.800	1.266	1.130	0.122	1.104	0.099
372.200	53596.800	1.224	1.177	0.163	1.142	0.133
357.300	51451.200	1.185	1.226	0.204	1.180	0.165
343.000	49392.000	1.146	1.278	0.245	1.220	0.199
329.300	47419.200	1.109	1.331	0.286	1.261	0.232
316.100	45518.400	1.073	1.386	0.327	1.303	0.265
303.500	43704.000	1.038	1.444	0.367	1.347	0.298
291.300	41947.200	1.004	1.504	0.408	1.392	0.331
279.700	40276.800	0.972	1.567	0.449	1.439	0.364
268.500	38664.000	0.940	1.632	0.490	1.487	0.397
257.700	37108.800	0.910	1.700	0.531	1.537	0.430
247.400	35625.600	0.880	1.771	0.572	1.588	0.463
237.500	34200.000	0.852	1.845	0.613	1.642	0.496

Table A-1: Peng-Robinson Isentropic expansion data

P-psia	P - lb/ft²	Density lb/ft³	Po/P	ln(Po/P)	V/Vo	ln(V/Vo)
438.20	63100.80	1.385	1.00	0.00	1.00	0.00
420.70	60580.80	1.340	1.04	0.04	1.03	0.03
403.80	58147.20	1.297	1.09	0.08	1.07	0.07
387.70	55828.80	1.255	1.13	0.12	1.10	0.10
372.20	53596.80	1.214	1.18	0.16	1.14	0.13
357.30	51451.20	1.175	1.23	0.20	1.18	0.16
343.00	49392.00	1.137	1.28	0.24	1.22	0.20
329.30	47419.20	1.100	1.33	0.29	1.26	0.23
316.10	45518.40	1.065	1.39	0.33	1.30	0.26
303.50	43704.00	1.030	1.44	0.37	1.34	0.30
291.30	41947.20	0.997	1.50	0.41	1.39	0.33
279.70	40276.80	0.965	1.57	0.45	1.44	0.36
268.50	38664.00	0.934	1.63	0.49	1.48	0.39
257.70	37108.80	0.904	1.70	0.53	1.53	0.43
247.40	35625.60	0.874	1.77	0.57	1.58	0.46
237.500	34200.00	0.846	1.85	0.61	1.64	0.49

Table A-2: Redlich-Kwong Isentropic expansion data

P-psia	P - lb/ft²	Density lb/ft³	Po/P	ln(Po/P)	V/Vo	ln(V/Vo)
438.20	63100.80	1.388	1.00	0.00	1.00	0.00
420.70	60580.80	1.343	1.04	0.04	1.03	0.03
403.80	58147.20	1.300	1.09	0.08	1.07	0.07
387.70	55828.80	1.258	1.13	0.12	1.10	0.10
372.20	53596.80	1.217	1.18	0.16	1.14	0.13
357.30	51451.20	1.178	1.23	0.20	1.18	0.16
343.00	49392.00	1.139	1.28	0.24	1.22	0.20
329.30	47419.20	1.103	1.33	0.29	1.26	0.23
316.10	45518.40	1.067	1.39	0.33	1.30	0.26
303.50	43704.00	1.032	1.44	0.37	1.34	0.30
291.30	41947.20	0.999	1.50	0.41	1.39	0.33
279.70	40276.80	0.967	1.57	0.45	1.44	0.36
268.50	38664.00	0.935	1.63	0.49	1.48	0.39
257.70	37108.80	0.905	1.70	0.53	1.53	0.43
247.40	35625.60	0.876	1.77	0.57	1.58	0.46
237.50	34200.00	0.848	1.85	0.61	1.64	0.49

Table A-3: Soave Redlich-Kwong Isentropic expansion data